

The Coulomb-Sturmian basis for the nuclear many-body problem

M. A. Caprio

Department of Physics, University of Notre Dame, Notre Dame, Indiana 46556-5670, USA

P. Maris and J. P. Vary

Department of Physics and Astronomy, Iowa State University, Ames, Iowa 50011-3160, USA

(Dated: August 22, 2012)

Calculations in *ab initio* no-core configuration interaction (NCCI) approaches, such as the no-core shell model (NCSM) or no-core full configuration (NCFC) methods, have conventionally been carried out using the harmonic-oscillator many-body basis. However, the rapid falloff (Gaussian asymptotics) of the oscillator functions at large radius makes them poorly suited for the description of the asymptotic properties of the nuclear wavefunction. We establish the foundations for carrying out NCCI calculations with an alternative many-body basis built from Coulomb-Sturmian functions. These provide a complete, discrete set of functions with a realistic exponential falloff. We present illustrative NCCI calculations for ${}^6\text{Li}$ with a Coulomb-Sturmian basis and investigate the center-of-mass separation and spurious excitations.

PACS numbers: 21.60.Cs, 21.10.-k, 27.20.+n, 02.30.Gp

I. INTRODUCTION

The combination of powerful theoretical frameworks with modern computing capabilities are making possible significant advances towards one of the basic goals of nuclear theory, namely, an *ab initio* understanding of the nucleus directly as a system of interacting protons and neutrons with realistic interactions. Nuclear interactions motivated by quantum chromodynamics are being developed, via effective field theory methods [1, 2], to provide an underlying Hamiltonian for the problem. It is then necessary to solve the nuclear many-body problem for this Hamiltonian, obtaining nuclear eigenstates and predictions for observables. In a no-core configuration interaction (NCCI) approach, such as the no-core shell model (NCSM) [3], the eigenproblem is formulated as a matrix diagonalization problem, in which the Hamiltonian matrix is represented with respect to a basis of antisymmetrized products of single-particle states. The nuclear eigenproblem is then solved for the full A -body system of nucleons, *i.e.*, there is no assumption of an inert core.

In practice, NCCI calculations have been based almost exclusively on a harmonic oscillator basis. In this article, we consider instead an alternative basis for the NCCI approach, built from Coulomb-Sturmian functions [4, 5]. These functions have previously been applied to few-body problems in atomic [4, 6–8] and hadronic [9–12] physics. The Coulomb-Sturmian functions have the distinctive property of constituting a complete, discrete set of square-integrable functions, while also possessing realistic exponential asymptotics appropriate to the nuclear problem. In the present work, the foundations for carrying out nuclear many-body calculations with the Coulomb-Sturmian basis are established. Then, illustrative calculations for the nucleus ${}^6\text{Li}$ are carried out

with the NCCI approach in a Coulomb-Sturmian basis.¹ Many of the considerations addressed here specifically in the context of the Coulomb-Sturmian basis are more broadly applicable to alternative single-particle bases for the nuclear problem.

Actual NCCI calculations must be carried out in a finite, truncated space. Progress in expanding the domain of applicability of the method is hampered by a combinatorial scale explosion in the dimension of the problem, with increasing size of the included space of single-particle states and with the number of nucleons in the system. The challenge is to reach a reasonable approximation of the converged results which would be achieved in the full, untruncated space for the many-body system. The success of the calculation is determined by the rate of convergence of calculated observables (energies, charge or mass radii, electromagnetic moments and transition rates, *etc.*) with increasing basis size and the ability to reliably extrapolate these results for finite spaces to the full many-body space [13–15]. Convergence rates may be expected to be sensitive to the choice of single-particle states from which the NCCI many-body basis is constructed, as well as the truncation scheme used for the many-body basis.

Before considering alternative bases, it is worth noting that the oscillator functions present significant advantages as a basis for the nuclear problem, which require

¹ The Coulomb-Sturmian single-particle states used in the present calculations arise as solutions to a general Sturm-Liouville equation (Sec. III A), rather than a Schrödinger equation or Hartree-Fock problem. They consequently do not physically correspond to “shells” in the conventional sense, *i.e.*, orbitals for independent-particle motion in some mean-field potential describing the zeroth-order dynamics of the system. Therefore, we use the more inclusive term *configuration interaction*, rather than specifically *shell model*, throughout the present work.

further assessment in moving to another basis:

(1) An exact factorization of center-of-mass and intrinsic wavefunctions is obtained in many-body calculations when the oscillator basis is used in conjunction with the N_{\max} truncation scheme (see Sec. II C), which is based on the total number of oscillator quanta. Thus, the oscillator basis with this truncation allows precise removal of or correction for spurious center-of-mass contributions to the dynamics.

(2) Matrix elements of the nucleon-nucleon two-body interaction are naturally formulated in the relative oscillator basis, of functions $\Psi_{nl}(\mathbf{r}_1 - \mathbf{r}_2)$ (see Sec. II A). These matrix elements can easily be transformed to the two-body oscillator basis, of functions $\Psi_{n_1 l_1}(\mathbf{r}_1) \Psi_{n_2 l_2}(\mathbf{r}_2)$, by the Moshinsky transformation [16]. The simplicity of this transformation is lost with any other single-particle basis. This is a fundamental concern, since the starting point of the many-body calculation is evaluation of the two-body matrix elements. (Similar comments apply for three-body or higher-body interactions.)

(3) The oscillator functions constitute a complete *discrete* basis for square-integrable functions. Many alternative bases do not provide this convenience. For instance, the bound state eigenfunctions of the Schrödinger equation for *finite-depth* potentials, such as the Woods-Saxon potential, are typically finite in number and in general do not constitute a complete set of square-integrable functions, without inclusion of the unbound continuum Schrödinger equation solutions as well.

Nonetheless, there are also strong reasons to consider moving beyond the oscillator basis. The classic and long-recognized (*e.g.*, Ref. [17]) physical limitation of the oscillator basis, for application to the nuclear problem, lies in the Gaussian falloff ($\propto e^{-\alpha r^2}$) at large distance r , which is a consequence of the quadratic confining harmonic oscillator potential. In contrast, for particles bound by a finite-range force, the actual asymptotics are exponential ($\propto e^{-\beta r}$). This mismatch in asymptotics, *i.e.*, the wavefunction tails, between the expansion basis and the physical system imposes a serious handicap on the convergence of calculations with increasing basis size. The problem is especially significant for observables, such as the root-mean-square radius or $E2$ strengths, which are sensitive to the large- r properties of the nuclear wavefunctions.

To adapt the Coulomb-Sturmian basis to the nuclear many-body problem, we must overcome the aforementioned technical challenges of moving away from the oscillator basis. The Coulomb-Sturmian functions, as already noted, are complete and offer the convenience of being a discrete set. The remaining challenges — transformation of matrix elements and center-of-mass factorization or spuriousity — are found to be tractable. First, we review the relevant aspects of the NCCI approach as conventionally implemented, including the oscillator single-particle basis (Sec. II A), the Hamiltonian (Sec. II B), and the N_{\max} many-body truncation scheme (Sec. II C). Then, procedures and results are established for using

the Coulomb-Sturmian basis for nuclear many-body calculations. The Coulomb-Sturmian functions are defined (Sec. III A), practicalities related to the radial length parameter are considered (Sec. III B), the transformation of interaction two-body matrix elements from the oscillator basis to the Coulomb-Sturmian basis is addressed (Sec. III C), and it is shown how the two-body matrix elements of the relative kinetic energy (and certain other operators) can be evaluated via separability (Sec. III D). Finally, illustrative NCCI calculations for ${}^6\text{Li}$ with the Coulomb-Sturmian basis (Sec. IV A) are compared with oscillator-basis calculations of the same dimensionality. The convergence of energies (Sec. IV B) and the root-mean-square radius (Sec. IV C) is examined, and issues of center-of-mass factorization and spurious states are explored in detail (Sec. IV D). Preliminary results were reported in Ref. [18].

II. BACKGROUND: NO-CORE SHELL MODEL

A. Harmonic-oscillator basis

The basis states conventionally used in the NCCI approach are antisymmetrized products of single-particle harmonic oscillator states. These single-particle states are eigenstates of the Hamiltonian

$$\hbar\Omega = \frac{p^2}{2m_N} + \frac{m_N\Omega^2 r^2}{2}, \quad (1)$$

where Ω denotes the oscillator frequency and m_N the nucleon mass, and \mathbf{r} and \mathbf{p} are the single-particle coordinates and momenta. For the spatial part of the solution, we have the usual three-dimensional oscillator wavefunctions

$$\Psi_{nlm}(\mathbf{r}) = N_{nl}(r/b)^l L_n^{l+1/2}[(r/b)^2] e^{-(r/b)^2/2} Y_{lm}(\hat{\mathbf{r}}), \quad (2)$$

with normalization factor

$$N_{nl} = \frac{1}{b^{3/2}} \left[\frac{2n!}{(l+n+1/2)!} \right]^{1/2}, \quad (3)$$

where the L_n^α are generalized Laguerre polynomials, the Y_{lm} are spherical harmonics, n is the radial quantum number, l and m are the orbital angular momentum and z -projection, and b is the oscillator length, given by $b = [\hbar/(m_N\Omega)]^{1/2}$. We use factorial notation $[x]! \equiv \Gamma(x+1)$ uniformly, for both integer and half-integer arguments. Letting $\Psi_{nlm}(\mathbf{r}) = r^{-1} R_{nl}(r) Y_{lm}(\hat{\mathbf{r}})$, the radial wavefunction is thus

$$R_{nl}(r) = b N_{nl}(r/b)^{l+1} L_n^{l+1/2}[(r/b)^2] e^{-(r/b)^2/2}. \quad (4)$$

The functions R_{nl} form an orthonormal set, with $\int_0^\infty dr R_{n'l}(r) R_{nl}(r) = \delta_{n'n}$. The full single-particle states $|nljm\rangle$, including spatial and spin degrees of freedom, are defined as usual for the nuclear shell model,

by coupling the orbital and spin- $\frac{1}{2}$ angular momenta to good total angular momentum j , with its z -projection again denoted by m .

The many-body basis states, for calculations in a space of fixed total many-body angular momentum projection M (M -scheme basis), are then

$$\psi = \mathcal{A}|n_1 l_1 j_1 m_1\rangle |n_2 l_2 j_2 m_2\rangle \cdots |n_A l_A j_A m_A\rangle, \quad (5)$$

where the operator \mathcal{A} represents antisymmetrization, over protons and neutrons separately. The many-body basis states are thus eigenstates of the Hamiltonian for noninteracting particles in a harmonic oscillator potential, $H^\Omega = \sum_i h_i^\Omega$. These states may be classified according to the total number of oscillator quanta $N_{\text{tot}} = \sum_i N_i = \sum_i (2n_i + l_i)$ and have energy eigenvalue $E = (N_{\text{tot}} + \frac{3}{2})A\hbar\Omega$ with respect to H^Ω . Thus, truncations by N_{tot} , as considered in the following section, are energy truncations under this noninteracting Hamiltonian.

Since we will later need to consider momentum-space wavefunctions, note that these are obtained as the Fourier transform

$$\tilde{\Psi}_{nlm}(\mathbf{k}) \equiv (2\pi)^{-3/2} \int d^3\mathbf{r} e^{-i\mathbf{k}\cdot\mathbf{r}} \Psi_{nlm}(\mathbf{r}). \quad (6)$$

The radial wavefunction \tilde{R}_{nl} in momentum space is defined by

$$\tilde{\Psi}_{nlm}(\mathbf{k}) = (-i)^l \frac{\tilde{R}_{nl}(k)}{k} Y_{lm}(\hat{\mathbf{k}}) \quad (7)$$

and is obtained as the Fourier-Bessel transform [19]

$$\tilde{R}_{nl}(k) = (2/\pi)^{1/2} \int_0^\infty dr kr j_l(kr) R_{nl}(r). \quad (8)$$

For the oscillator, \tilde{R}_{nl} has the same functional form as the coordinate-space oscillator wavefunction R_{nl} , with [5]

$$\tilde{R}_{nl}(k) = (-)^n \frac{1}{b} \tilde{N}_{nl}(bk)^{l+1} L_n^{l+1/2}[(bk)^2] e^{-(bk)^2/2}, \quad (9)$$

where

$$\tilde{N}_{nl} = b^{3/2} \left[\frac{2n!}{(l+n+1/2)!} \right]^{1/2}. \quad (10)$$

The \tilde{R}_{nl} form an orthonormal set, with $\int_0^\infty dk \tilde{R}_{n'l}(k) \tilde{R}_{nl}(k) = \delta_{n'l}$.

B. Hamiltonian

We now review the properties of the nuclear Hamiltonian which are most relevant to understanding the solution method based on the Coulomb-Sturmian basis (Sec. III) and the results from applying this method (Sec. IV). The NCCI approach is based upon a nonrelativistic nuclear many-body Hamiltonian of the form

$$H = T + V, \quad (11)$$

where T is the one-body kinetic energy operator and V represents the interaction of the nucleons. Commonly, the isoscalar kinetic energy

$$T = \frac{1}{2m_N} \sum_i p_i^2 \quad (12)$$

is used, that is, protons and neutrons are treated equivalently as having the average nucleon mass m_N , and the summation index i runs over all A nucleons. The potential V is a Galilean-invariant operator involving two-body and possibly higher many-body terms.

The Hamiltonian (11) has the essential property that it may be separated into center-of-mass and intrinsic (Galilean-invariant) contributions. The kinetic energy operator separates into a term

$$T_{\text{c.m.}} = \frac{1}{2Am_N} \left(\sum_i \mathbf{p}_i \right)^2 = \frac{P^2}{2Am_N} \quad (13)$$

representing the center-of-mass kinetic energy and a term

$$T_{\text{rel}} = \frac{1}{4Am_N} \sum'_{ij} (\mathbf{p}_i - \mathbf{p}_j)^2 = \frac{p_{\text{rel}}^2}{2Am_N} \quad (14)$$

representing the kinetic energy of relative motion of the nucleons, where the prime on the summation \sum'_{ij} indicates $i \neq j$. The decomposition of both the r^2 and p^2 operators into center-of-mass and relative contributions is summarized in Appendix A, which also serves to define a uniform notation for the present work. The operator T_{rel} depends only upon relative momenta $\mathbf{p}_i - \mathbf{p}_j$ and is therefore Galilean invariant. Thus, the full nuclear Hamiltonian (11) may be separated as $H = T_{\text{c.m.}} + H_{\text{in}}$, where

$$H_{\text{in}} = T_{\text{rel}} + V \quad (15)$$

is the Galilean-invariant *intrinsic Hamiltonian*. As a consequence of the separability of H , a complete set of eigenstates may be found with coordinate-space wavefunctions which have the factorized form

$$\psi(\mathbf{r}_i; \boldsymbol{\sigma}_i) = \psi_{\text{c.m.}}(\mathbf{R}) \psi_{\text{in},k}(\mathbf{r}_{ij}; \boldsymbol{\sigma}_i). \quad (16)$$

The factor $\psi_{\text{c.m.}}(\mathbf{R})$ depends only on the center-of-mass coordinate, and the factor $\psi_{\text{in},k}(\mathbf{r}_{ij}; \boldsymbol{\sigma}_i)$ depends only on relative coordinates $\mathbf{r}_{ij} = \mathbf{r}_i - \mathbf{r}_j$ and intrinsic spin degrees of freedom, indicated schematically here by the arguments $\boldsymbol{\sigma}_i$. For each intrinsic excitation, with wavefunction ψ_{in} , an infinite set of eigenstates sharing this same intrinsic structure but different center-of-mass excitations $\psi_{\text{c.m.}}$ is obtained. The corresponding energy eigenvalue separates into eigenvalues of $T_{\text{c.m.}}$ and H_{in} , as $E = E_{\text{c.m.}} + E_{\text{in}}$.

The “interesting” many-body spectroscopy of the nucleus resides in the intrinsic wavefunctions ψ_{in} and eigenvalues E_{in} , but the “uninteresting” center-of-mass motion remains as an unavoidable and potentially obfuscating element of the solution. In principle, the center-of-mass motion may be completely eliminated from the

problem, by explicitly changing variables to relative coordinates. However, the nuclear many-body state must be antisymmetrized, and this process rapidly becomes intractable with increasing nucleon number. On the other hand, if we instead solve the nuclear eigenproblem in a many-body basis constructed from antisymmetrized products of single-particle states, antisymmetrization is straightforward, but we are consigned to simultaneously solving for center-of-mass and intrinsic excitations.

Before we consider the specifics of formulating the eigenproblem with respect to a basis, it is worth considering the solutions in the full coordinate space further. First, it is convenient to remove the complication of the center-of-mass kinetic energy operator, by considering the eigenproblem not for the full Hamiltonian H of (11) but rather for the intrinsic Hamiltonian H_{in} of (15). The full spectroscopic information of the original problem is maintained, since the eigenstates still have wavefunctions of the form $\psi(\mathbf{r}_i; \boldsymbol{\sigma}_i) = \psi_{\text{c.m.}}(\mathbf{R})\psi_{\text{in}}(\mathbf{r}_{ij}; \boldsymbol{\sigma}_i)$, but these are now simply associated with eigenvalues $E = E_{\text{in}}$. Thus, for each intrinsic wavefunction ψ_{in} , an infinite set of eigenstates sharing the same intrinsic structure but different center-of-mass excitations $\psi_{\text{c.m.}}$ is still obtained, and these are now strictly degenerate with each other.

Since $T_{\text{c.m.}}$ has been eliminated from the Hamiltonian, we are free to consider any complete set of wavefunctions to span the degenerate space of center-of-mass wavefunctions. For instance, suppose plane wave solutions $\psi_{\text{c.m.}}(\mathbf{R}) = e^{-i\mathbf{K}\cdot\mathbf{R}}$ are taken for the center of mass. Then, for each intrinsic excitation $\psi_{\text{in},k}$, with intrinsic eigenvalue E_k , a continuum of eigenstates will be obtained, having wavefunctions $\psi(\mathbf{r}_i; \boldsymbol{\sigma}_i) = e^{-i\mathbf{K}\cdot\mathbf{R}}\psi_{\text{in},k}(\mathbf{r}_{ij}; \boldsymbol{\sigma}_i)$. Under the full Hamiltonian H , these states form a continuum with $E = \hbar^2 K^2 / (2Am_N) + E_k$, but, under H_{in} , these states are infinitely degenerate, all with $E = E_k$.

Although they provide the simplest illustration, plane wave center-of-mass wavefunctions do not naturally occur in our actual solutions to the eigenproblem, which are obtained in terms of *spatially localized* single-particle basis wavefunctions. The choice of basis for center-of-mass wavefunctions with direct practical significance in oscillator-basis calculations consists instead of three-dimensional harmonic oscillator wavefunctions, $\psi_{\text{c.m.}}(\mathbf{R}) = \Psi_{nlm}(\mathbf{R})$. The $\Psi_{nlm}(\mathbf{R})$ are eigenfunctions of the center-of-mass harmonic oscillator Hamiltonian $H_{\text{c.m.}}^\Omega$, defined with oscillator frequency Ω and mass Am_N , i.e.,

$$H_{\text{c.m.}}^\Omega = T_{\text{c.m.}} + \frac{Am_N\Omega^2 R^2}{2}. \quad (17)$$

The center-of-mass excitation is thus characterized by the number $N_{\text{c.m.}} = 2n + l$ of oscillator quanta. This particular choice of center-of-mass wavefunctions is enforced as the eigenstates of the Hamiltonian, if the degeneracy of center-of-mass states is broken by introducing a *Lawson term* [20] proportional to $H_{\text{c.m.}}^\Omega$. It is both conventional and convenient to subtract the zero-

point energy of center-of-mass motion with respect to this term, so the Lawson term has the form $\lambda(H_{\text{c.m.}}^\Omega - \frac{3}{2}\hbar\Omega)$, with λ positive, or, more transparently, $aN_{\text{c.m.}}^\Omega$, where $N_{\text{c.m.}}^\Omega = (H_{\text{c.m.}}^\Omega - \frac{3}{2}\hbar\Omega)/(\hbar\Omega)$ is the number operator associated with (17). The Hamiltonian thus becomes

$$H = T_{\text{rel}} + V + aN_{\text{c.m.}}^\Omega. \quad (18)$$

The factorized eigenstates have coordinate space wavefunctions $\psi(\mathbf{r}_i; \boldsymbol{\sigma}_i) = \Psi_{nlm}(\mathbf{R})\psi_{\text{in}}(\mathbf{r}_{ij}; \boldsymbol{\sigma}_i)$, and the eigenvalues are now $E = E_k + aN_{\text{c.m.}}^\Omega$. Thus, the eigenvalues for states with $N_{\text{c.m.}} = 0$ are unchanged by the Lawson term, still simply the intrinsic energies E_k , while the eigenvalues of spurious states, with $N_{\text{c.m.}} > 0$, are raised out of the low-lying spectrum, to an excitation energy of at least a .

C. Many-body N_{max} truncation

The factorization of the wavefunction just described is possible in the full space of the many-body system. However, in practice, diagonalization of the Hamiltonian must be carried out in a finite-dimensional subspace spanned by some truncated basis. In general, one cannot expect to be able to construct center-of-mass factorized states in such a subspace. The separation $\psi(\mathbf{r}_i; \boldsymbol{\sigma}_i) = \psi_{\text{c.m.}}(\mathbf{R})\psi_{\text{in}}(\mathbf{r}_{ij}; \boldsymbol{\sigma}_i)$ will be lost, and it will not be possible to divide the set of eigenstates into “non-spurious” states, consisting of a simple product of a 0s center-of-mass wavefunction with a single intrinsic excitation, and “spurious” states, involving center-of-mass excitations. However, there is an important special case in which factorization occurs, namely, for a harmonic-oscillator many-body basis in the so-called N_{max} truncation scheme, which is based on the total number of oscillator quanta for the many-body state. This truncation is commonly used in NCCI calculations. In this section, we briefly examine the structure of the N_{max} -truncated space, both to understand what changes as we go to a general single-particle basis and as a prerequisite to understanding the spurious state spectrum observed for NCCI calculations with the Coulomb-Sturmian basis in Sec. IV D.

Factorization is to be expected if the truncated space \mathcal{H} for the calculation has a simple product structure, before antisymmetrization,²

$$\mathcal{H} = \mathcal{H}_{\text{c.m.}} \otimes \mathcal{H}_{\text{in}}. \quad (19)$$

² If the truncated space has the form $\mathcal{H}_{\text{c.m.}} \otimes \mathcal{H}_{\text{in}}$, it is in principle possible to choose a basis consisting of product functions $\phi_{\text{c.m.},i}\phi_{\text{in},j}$. Since H_{in} acts only on intrinsic degrees of freedom, it does not connect basis states involving different $\phi_{\text{c.m.},i}$. Therefore, the Hamiltonian matrix with respect to this basis is block diagonal, with each block simply consisting of the matrix representation of H_{in} on the basis of intrinsic states $\phi_{\text{in},j}$.

Most simply, if all nucleons are restricted to occupy a filled core plus valence orbitals taken from a *single* major oscillator shell, the many-body space does factorize in the form (19), with pure 0s motion for the center of mass, as shown by Elliott and Skyrme [21]. The essential reason is that the total number N_{tot} of harmonic oscillator quanta is identical whether calculated as the sum of single particle oscillator quanta, $N_{\text{tot}} = \sum_i N_i$, or as the sum of center-of-mass and intrinsic quanta $N_{\text{tot}} = N_{\text{c.m.}} + N_{\text{in}}$ [21]. The equivalence may be seen from the decomposition of the one-body number operator $N = (\hbar\Omega)^{-1}[p^2/(2m_N) + (m_N\Omega^2/2)r^2 - 3\hbar\Omega/2]$ into center-of-mass and intrinsic parts (which follows from Appendix A). Thus, the space for this situation is $\mathcal{H}^0 = \mathcal{H}_{\text{c.m.}}^0 \otimes \mathcal{H}_{\text{in}}^0$, where $\mathcal{H}_{\text{c.m.}}^0$ is the one-dimensional space containing the 0s oscillator function, and $\mathcal{H}_{\text{in}}^0$ is the space of intrinsic functions with no excitations above the valence shell.

The N_{max} truncation scheme is a generalization, which likewise yields factorized eigenstates. Consider a space spanned by product states subject to the truncation

$$N_{\text{tot}} = \sum_i N_i \leq N_0 + N_{\text{max}}, \quad (20)$$

where N_0 is the minimal number of oscillator quanta for the given number of protons and neutrons, if all nucleons occupy the lowest permitted shells. (The Elliott and Skyrme space described above is obtained for $N_{\text{max}} = 0$.) The N_{max} -truncated space may be decomposed as a direct sum of product spaces, before antisymmetrization,³

$$\begin{aligned} \mathcal{H}^{N_{\text{max}}} = & \mathcal{H}_{\text{c.m.}}^0 \otimes \mathcal{H}_{\text{in}}^{N_{\text{max}}} + \mathcal{H}_{\text{c.m.}}^1 \otimes \mathcal{H}_{\text{in}}^{N_{\text{max}}-1} \\ & + \mathcal{H}_{\text{c.m.}}^2 \otimes \mathcal{H}_{\text{in}}^{N_{\text{max}}-2} + \dots + \mathcal{H}_{\text{c.m.}}^{N_{\text{max}}} \otimes \mathcal{H}_{\text{in}}^0, \end{aligned} \quad (21)$$

where $\mathcal{H}_{\text{c.m.}}^N$ is the space of center-of-mass functions with exactly N oscillator quanta, and $\mathcal{H}_{\text{in}}^N$ is the space of intrinsic functions with N or fewer intrinsic excitation quanta above N_0 . Consequently, factorization is maintained, but, in the solution to the many-body problem in an N_{max} -truncated space, several approximate copies of the intrinsic spectroscopy are obtained, each in a more highly-truncated space. The $\mathcal{H}_{\text{c.m.}}^0 \otimes \mathcal{H}_{\text{in}}^{N_{\text{max}}}$ block yields the “interesting” solutions, or nonspurious states, consisting of a 0s center-of-mass function multiplied by the solutions in the least-truncated intrinsic space $\mathcal{H}_{\text{in}}^{N_{\text{max}}}$.

Then the $\mathcal{H}_{\text{c.m.}}^1 \otimes \mathcal{H}_{\text{in}}^{N_{\text{max}}-1}$ block yields a 0p center-of-mass function multiplied by the solutions of the intrinsic problem in the $\mathcal{H}_{\text{in}}^{N_{\text{max}}-1}$ space, the $\mathcal{H}_{\text{c.m.}}^2 \otimes \mathcal{H}_{\text{in}}^{N_{\text{max}}-2}$ block yields 1s and 0d center-of-mass functions multiplied by the solutions of the intrinsic problem in the $\mathcal{H}_{\text{in}}^{N_{\text{max}}-2}$ space, *etc.* In actual calculations, these “uninteresting” solutions, or spurious states, may be identified by evaluating the expectation value $\langle N_{\text{c.m.}}^\Omega \rangle$.

The presence of such spurious states in the low-lying calculated spectrum has considerable practical implications. Although these states are clearly identifiable, as noted, diagonalization of such large matrices as encountered in NCCI calculations typically relies upon methods such as the Lanczos algorithm [22], which efficiently extract a selected set of energy eigenvalues (and corresponding eigenvectors), namely, those lowest in the energy spectrum. With increasing N_{max} , the low-energy spectrum would be increasingly cluttered with spurious states (as illustrated more concretely in Sec. IV D), limiting the ability of the Lanczos diagonalization to access the low-lying intrinsic excited states. The spurious states are therefore, in practice, typically shifted to higher energy by inclusion of a Lawson term (Sec. II B) in the Hamiltonian, so that they do not interfere with the low-lying spectrum obtained by diagonalization.

As a final practical matter, it is necessary to note that, for calculations with parity-conserving nuclear interactions, the N_{max} truncation of (20) is further restricted either to N_{tot} even or to N_{tot} odd. If, *e.g.*, even N_{tot} are taken, so $\mathcal{H}^{N_{\text{max}}}$ is the even-parity space for the nucleus, then the $\mathcal{H}_{\text{c.m.}}^0 \otimes \mathcal{H}_{\text{in}}^{N_{\text{max}}}$ subspace yields only even-parity intrinsic excitations, the $\mathcal{H}_{\text{c.m.}}^1 \otimes \mathcal{H}_{\text{in}}^{N_{\text{max}}-1}$ subspace yields the odd-parity 0p center-of-mass function multiplied by odd-parity intrinsic excitations, the $\mathcal{H}_{\text{c.m.}}^2 \otimes \mathcal{H}_{\text{in}}^{N_{\text{max}}-2}$ subspace yields the even-parity intrinsic excitations again but evaluated in the smaller $N_{\text{max}} - 2$ intrinsic space, *etc.*

III. THE COULOMB-STURMIAN BASIS

A. Coulomb-Sturmian functions

The harmonic oscillator functions have the desirable properties, as basis functions for an eigenfunction expansion, that these form a complete *discrete* set (of square-integrable functions on \mathbb{R}^3), *i.e.*, without a continuum. However, the oscillator functions are obtained from an infinitely bound potential and decay with Gaussian ($e^{-\alpha r^2}$) asymptotics, *i.e.*, they satisfy an undesirable boundary condition for problems involving finite binding. Conversely, the Schrödinger equation for the Coulomb potential yields a set of eigenfunctions which have exponentially decaying asymptotics ($e^{-\beta r}$), as desired, but which do not form a complete set (of square-integrable functions on \mathbb{R}^3) unless the positive-energy continuum Coulomb wavefunctions are included. However, a closely related set of functions, the *Coulomb-Sturmian* func-

³ Since the N_{max} -truncated space has the form (21), it is in principle possible to obtain a basis for $\mathcal{H}^{N_{\text{max}}}$ consisting of products of the form $\phi_{\text{c.m.},i}^{N_{\text{c.m.}}} \phi_{\text{in},j}^{N_{\text{max}}-N_{\text{c.m.}}}$. (The actual basis used in NCCI calculations need not be, and generally is not, of this form.) Since H_{in} does not connect basis states involving different center-of-mass wavefunctions, the Hamiltonian matrix with respect to this basis is block diagonal, with each block, corresponding to a given $\phi_{\text{c.m.},i}^{N_{\text{c.m.}}}$, simply consisting of the matrix representation of H_{in} on the basis of intrinsic states for $\mathcal{H}_{\text{in}}^{N_{\text{max}}-N_{\text{c.m.}}}$.

tions [4–6, 8, 11], can be obtained as the solutions to a Sturm-Liouville problem associated with the Coulomb potential. These functions retain the exponential asymptotics of the Coulomb problem while also forming, in the final form in which we will write them, a complete and *discrete* set of square-integrable functions on \mathbb{R}^3 . The Coulomb-Sturmian functions thus combine favorable attributes of both the oscillator and Coulomb functions, as an expansion basis for three-dimensional Schrödinger problems.

To begin with, let us recall the Schrödinger equation solutions for the Coulomb potential. The functions

$$W_{nlm}(\mathbf{r}) = N_{nl} \left(\frac{2r}{n+l+1} \right)^l \times L_n^{2l+1} \left(\frac{2r}{n+l+1} \right) e^{-r/(n+l+1)} Y_{lm}(\hat{\mathbf{r}}), \quad (22)$$

with

$$N_{nl} = \left(\frac{2}{n+l+1} \right)^{3/2} \left[\frac{n!}{2(n+l+1)(n+2l+1)!} \right]^{1/2}, \quad (23)$$

satisfy the Schrödinger equation

$$\left(-\nabla^2 - \frac{2}{r} - 2E_{nl} \right) W(\mathbf{r}) = 0, \quad (24)$$

with energy eigenvalue

$$E_{nl} = -\frac{1}{2(n+l+1)^2}. \quad (25)$$

This is the Schrödinger equation, written in dimensionless form ($\hbar^2/m = 1$), for the potential $V(r) = 1/r$. The functions W are orthonormal with respect to the standard inner product on \mathbb{R}^3 , that is,

$$\int d^3\mathbf{r} W_{n'l'm'}^*(\mathbf{r}) W_{nlm}(\mathbf{r}) = \delta_{(n'l'm')(nlm)}. \quad (26)$$

Observe that r always appears in the usual Coulomb functions divided by a scale $n+l+1$, which depends upon the quantum numbers n and l .⁴ The Coulomb-Sturmian functions are obtained by replacing $(n+l+1) \rightarrow b$ in (22), that is, by carrying out a radial change of variable on each function so as to obtain a constant length scale b , yielding

$$\Phi_{nlm}(\mathbf{r}) = N_{nl} (2r/b)^l L_n^{2l+1} (2r/b) e^{-r/b} Y_{lm}(\hat{\mathbf{r}}), \quad (27)$$

with

$$N_{nl} = \left(\frac{2}{b} \right)^{3/2} \left[\frac{n!}{2(n+l+1)(n+2l+1)!} \right]^{1/2}. \quad (28)$$

By making the same change of variable in (24), it is seen that the functions Φ satisfy

$$\left(-\nabla^2 + \frac{1}{b^2} - \alpha_{nl} \frac{2}{r} \right) \Phi(\mathbf{r}) = 0, \quad (29)$$

with eigenvalue $\alpha_{nl} = (n+l+1)/b$. They are thus solutions to a Sturm-Liouville eigenproblem, with the Coulomb potential as weighting function.⁵ The solutions $\Phi(\mathbf{r})$ consequently are orthogonal, with respect to the same weighting function. In particular,

$$\int d^3\mathbf{r} \Phi_{n'l'm'}^*(\mathbf{r}) \frac{1}{r} \Phi_{nlm}(\mathbf{r}) = \frac{1}{b(n+l+1)} \delta_{(n'l'm')(nlm)}. \quad (30)$$

Since (29) is obtained from the Schrödinger equation simply by a change of variable, the solutions Φ_{nlm} may also be considered [4] as a set of solutions to the Schrödinger equation. However, by comparison of (24) with (29), it is seen then that the *scale*, or depth, of the potential must be taken to vary with each solution, as α_{nl} , so the solutions to the problem share a constant *energy* $E_0 = -1/(2b^2)$, equal to the ground state energy E_{00} of the associated Schrödinger equation, from (25), after the substitution $(n+l+1) \rightarrow b$.

For use as an expansion basis in quantum mechanical problems, it is desirable to obtain a set of functions which are orthonormal with respect to the standard integration metric. This may be accomplished by absorbing the integration weight $1/r$ and norm $1/[b(n+l+1)]$ appearing in (30) into the Coulomb-Sturmian function itself, *i.e.*, multiplying the function Φ_{nlm} of (27) by $[b(n+l+1)/r]^{1/2}$. However, the radial dependence of the resulting functions involves a half-integral power of r , $\Phi \sim r^{l-1/2}$, for $r \rightarrow 0$. In contrast, the harmonic oscillator functions (2) have dependence $\Psi \sim r^l$ for $r \rightarrow 0$. We can recover this relation between the $r \rightarrow 0$ asymptotics and the angular momentum by furthermore shifting $l \rightarrow l+1/2$ in the radial part of the Coulomb-Sturmian functions, yielding new functions [5, 26]

$$\Lambda_{nlm}(\mathbf{r}) = N_{nl} (2r/b)^l L_n^{2l+2} (2r/b) e^{-r/b} Y_{lm}(\hat{\mathbf{r}}), \quad (31)$$

where now

$$N_{nl} = \left(\frac{2}{b} \right)^{3/2} \left[\frac{n!}{(n+2l+2)!} \right]^{1/2}. \quad (32)$$

⁴ The combination $n+l+1$ is in fact the *principal*, or energy, quantum number, which enters into the energy eigenvalue E_{nl} in (25). In comparing with the literature, it should be borne in mind that, traditionally, the principal quantum number for the Coulomb problem is denoted by n [23], and this notation propagates to some discussions of the Coulomb-Sturmian functions (*e.g.*, Refs. [4, 5]). However, consistency with conventional notation for the oscillator problem [16] and nuclear shell model [24] is strongly desirable in the present context. Hence, we reserve the symbol n for the radial quantum number ($n = 0, 1, \dots$).

⁵ More precisely, the one-dimensional radial equation associated with (29),

$$\left[-\frac{d^2}{dr^2} + \left(\frac{l(l+1)}{r^2} + \frac{1}{b^2} \right) - \alpha_{nl} \frac{2}{r} \right] \varphi(r) = 0,$$

obtained by setting $\Phi(\mathbf{r}) = r^{-1} \varphi(r) Y_{lm}(\hat{\mathbf{r}})$, has the form of a Sturm-Liouville equation $[(d/dr)p(r)(d/dr) + q(r) + \lambda w(r)]u(r) = 0$ [25], with weight function $w(r) \propto 1/r$.

Although both Φ_{nlm} and Λ_{nlm} are defined in terms of generalized Laguerre polynomials L_n^α , the polynomials appearing in the Φ_{nlm} have *odd* $\alpha = 2l + 1$, while those appearing in the Λ_{nlm} have *even* $\alpha = 2l + 2$. The functions $\Lambda(\mathbf{r})$ are orthogonal with respect to the standard inner product, *i.e.*,

$$\int d^3\mathbf{r} \Lambda_{n'l'm'}^*(\mathbf{r}) \Lambda_{nlm}(\mathbf{r}) = \delta_{(n'l'm')(nlm)}. \quad (33)$$

Moreover, they can be shown to form a complete set on the space of square-integrable functions on \mathbb{R}^3 [5, 27]. Letting $\Lambda_{nlm}(r) = r^{-1} S_{nl}(r) Y_{lm}(\hat{\mathbf{r}})$, the radial wavefunction for our Coulomb-Sturmian expansion basis is thus

$$S_{nl}(r) = (2/b)^{-1} N_{nl} (2r/b)^{l+1} L_n^{2l+2}(2r/b) e^{-r/b}. \quad (34)$$

The S_{nl} form an orthonormal set, with $\int_0^\infty dr S_{n'l}(r) S_{nl}(r) = \delta_{n'n}$.

The momentum-space representation of the Coulomb-Sturmian functions (as for Coulomb functions in general) may be evaluated analytically [5, 11]. This property of the basis is particularly useful, in the present application, for evaluation of matrix elements of the kinetic energy operators. The momentum-space wavefunction, defined as in (6)–(8), is simply expressed in terms of Jacobi polynomials. If we let $\tilde{\Lambda}_{nlm}(\mathbf{k}) = k^{-1} (-i)^l \tilde{S}_{nl}(k) Y_{lm}(\hat{\mathbf{k}})$, then

$$\tilde{S}_{nl}(k) = \frac{1}{b} \tilde{N}_{nl} \frac{(bk)^{l+1}}{[(bk)^2 + 1]^{l+2}} P_n^{(l+3/2, l+1/2)} \left[\frac{(bk)^2 - 1}{(bk)^2 + 1} \right], \quad (35)$$

with normalization factor

$$\tilde{N}_{nl} = 2b^{3/2} \frac{[n!(n+2l+2)!]^{1/2}}{(n+l+\frac{1}{2})!}. \quad (36)$$

The \tilde{S}_{nl} form an orthonormal set, with $\int_0^\infty dk \tilde{S}_{n'l}(k) \tilde{S}_{nl}(k) = \delta_{n'n}$.

B. Length parameter

For any given value of l , the radial wavefunctions $S_{nl}(r)$, with $n = 0, 1, \dots$, constitute a complete and orthogonal set on \mathbb{R}^+ , regardless of the choice of length scale parameter b in (34). For the full wavefunctions $\Lambda_{nlm}(\mathbf{r})$ on \mathbb{R}^3 , orthogonality of functions with *different* l quantum numbers is enforced by the $Y_{lm}(\hat{\mathbf{r}})$ factor, regardless of the radial wavefunction. Therefore, the choice of length parameter b may be made independently for each l -space, and orthogonality of the basis of single-particle states on \mathbb{R}^3 will still be preserved.⁶

The freedom to define distinct b_l , for different values of l , appears to be crucial to the present use of a Coulomb-Sturmian basis for the nuclear problem. A many-body basis built from oscillator wavefunctions has had considerable past success in providing a reasonable first approximation to the central portion of the wavefunctions in the nuclear problem and also clearly enjoys the advantage of complete separability of center-of-mass motion. As we introduce the Coulomb-Sturmian basis, we wish to retain the successes enjoyed by the oscillator basis, to the extent possible, while also now providing for exponential asymptotics in the tail, or large r , region.

If b is simply taken independent of l , Coulomb-Sturmian radial functions $S_{nl}(r)$ are obtained as shown in Fig. 1 (top). For illustration, we use the dimensionless value $b = 1$ for the length parameter. The first four radial functions ($0 \leq n \leq 3$) are shown as probability distributions $|S_{nl}(r)|^2$, for $l = 0$ [Fig. 1(a)], $l = 2$ [Fig. 1(b)], and $l = 8$ [Fig. 1(c)]. These functions may be compared with the corresponding radial functions $R_{nl}(r)$ for the harmonic oscillator, as shown in Fig. 1 (bottom), again taking the dimensionless value $b = 1$ for the length parameter. For the $S_{nl}(r)$, it may be observed that the radial probability distribution migrates rapidly to large r as l increases. By $l = 8$, the $n = 0$ function [Fig. 1(c)] shares virtually no overlap with the several lowest- n oscillator functions [Fig. 1(i)]. Physically, it is reasonable to expect that the success of the oscillator basis in describing the central portion of the nuclear wavefunction may be lost in such a basis. Convergence of the description of center-of-mass motion may also be compromised. Computationally, there is a purely pragmatic difficulty which effectively precludes calculations with such a basis. It will be seen in Sec. III C that significant overlaps between the low- n members of the Coulomb-Sturmian and oscillator bases are required, to carry out a change-of-basis transformation on the interaction matrix elements with reasonable accuracy.

We therefore seek an alternative prescription for b_l , which provides a closer alignment of the low- n Coulomb-Sturmian basis functions with the harmonic oscillator basis functions. A straightforward, though certainly not unique, solution is to choose b_l so as to align the node of the $n = 1$ Coulomb-Sturmian function, for the given value of l , with the node of the $n = 1$ oscillator function, for this same value of l . It is convenient to work in this fashion, with nodes rather than, say, maxima, since the nodes are given by the zeros of generalized Laguerre polynomials [28]. Let $x_{n,s}^\alpha$ denote the s th zero of the generalized Laguerre polynomial $L_n^\alpha(x)$. The condition obtained for b_l , relative to the oscillator length b_{HO} , is

$$\frac{b_l}{b_{\text{HO}}} = \frac{2(x_{1,1}^{l+1/2})^{1/2}}{x_{1,1}^{2l+2}}, \quad (37)$$

which yields the simple analytic result

$$\frac{b_l}{b_{\text{HO}}} = \sqrt{\frac{2}{2l+3}}. \quad (38)$$

⁶ In fact, when spin is introduced in the single-particle basis, a distinct value b_{lj} may be chosen for the length parameter independently for each lj -space, much as different sets of radial wavefunctions are obtained for each lj value in the shell model Woods-Saxon basis [24]. Different values may also be chosen for the proton and neutron spaces.

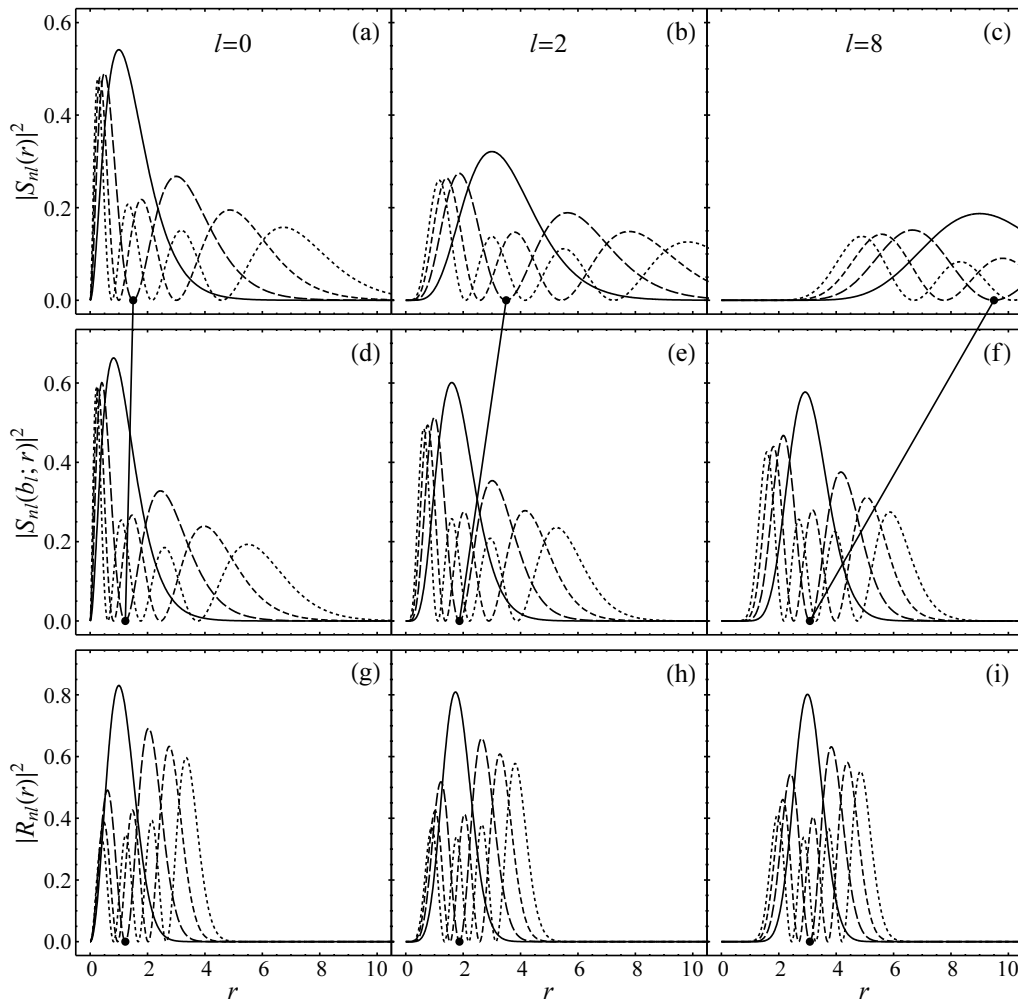


FIG. 1: Radial basis functions (shown as squared amplitudes), with $0 \leq n \leq 3$, for $l = 0$ (left), $l = 2$ (center), and $l = 8$ (right): (a–c) Coulomb-Sturmian functions $S_{nl}(r)$, with fixed length parameter $b = 1$, (d–f) rescaled Coulomb-Sturmian functions $S_{nl}(b_l; r)$, with l -dependent length parameter b_l given by the prescription (38), and (g–i) harmonic oscillator functions $R_{nl}(r)$, with fixed length parameter $b = 1 [\equiv b_{\text{HO}}]$. The dots mark the location of the node of the $n = 1$ function in each panel, and the connector lines highlight the shift in this node between the top and middle rows.

Thus, *e.g.*, $b_0/b_{\text{HO}} \approx 0.8165$, $b_1/b_{\text{HO}} \approx 0.6325$, and $b_2/b_{\text{HO}} \approx 0.5345$. The nodes under consideration are marked by dots in Fig. 1. Selecting b_l/b_{HO} according to (38) yields radially rescaled Coulomb-Sturmian functions as in Fig. 1 (middle). These functions are seen to provide a much closer match to the oscillator functions of Fig. 1 (bottom) in the small- r central region, than do the unscaled functions of Fig. 1 (top), while still retaining greater support than the oscillator functions in the large- r tail region.

The optimal approach to choosing the b_l may be expected to depend upon the problem at hand — nucleus, interaction, states of interest, observables of interest, and many-body truncation scheme in use — and warrants thorough investigation. The prescription (38) would appear to be a reasonable starting point and is therefore used in the example NCCI calculations of Sec. IV. How-

ever, it remains to be determined what prescription for b_l might ultimately yield the most rapid convergence in the many-body problem. Under some circumstances, it may even be appropriate to choose the b_l separately for the proton and neutron spaces, for instance, for neutron halo nuclei.

C. Transformation of matrix elements

For the many-body problem, we now consider a basis built up from the Coulomb-Sturmian functions Λ_{nlm} , combined with spin to give nlj states as usual. The angular and spin dependence is thus the same as for the harmonic oscillator single-particle states, but with the harmonic oscillator radial wavefunctions R_{nl} replaced by the S_{nl} . Many-body basis states may be built as anti-

symmetrized products of these single-particle states exactly as before, *i.e.*, according to (5). For the many-body calculation, it is necessary for one to evaluate the matrix elements of the Hamiltonian with respect to the many-body basis states. However, the specific choice of single-particle basis enters into the problem only through the two-body matrix elements of this Hamiltonian, if the interaction is limited to two-body contributions, or three-body matrix elements if a three-body interaction is considered, *etc.* Here we consider specifically two-body interactions and matrix elements, but the discussion readily generalizes to higher-body interactions.

If the two-body matrix elements of an interaction are known with respect to the oscillator basis, matrix elements with respect to the Coulomb-Sturmian basis may then be obtained by a straightforward sum over two-body states. Strong practical considerations suggest first generating the nuclear interaction two-body matrix elements in the oscillator representation. By Galilean invariance, the interaction itself is a function only of the relative $\mathbf{r}_2 - \mathbf{r}_1$ degree of freedom and the intrinsic spins. Conventionally, for NCCI calculations, the two-body interaction is first represented via its matrix elements in a basis of harmonic oscillator states in the relative spatial degree of freedom, coupled to the spins, *i.e.*, $|nl; SJ\rangle$. The transformation from a relative oscillator basis to a single-particle oscillator basis, *i.e.*, to product states $|n_a l_a j_a, n_b l_b j_b; J\rangle$ for the two-particle system, can then be carried out through the well-developed framework of the Moshinsky transformation [16]. Such a convenient means of transformation is not, in general, available for other bases.⁷ Therefore, only after this transformation to single-particle degrees of freedom do we carry out the transformation to the Coulomb-Sturmian basis.

For purposes of discussing the change of basis, let us label single-particle orbitals for the oscillator basis by unbarred symbols $a = (n_a l_a j_a)$, $b = (n_b l_b j_b)$, *etc.*, and those for the Coulomb-Sturmian basis by barred symbols $\bar{a} = (\bar{n}_a \bar{l}_a \bar{j}_a)$, $\bar{b} = (\bar{n}_b \bar{l}_b \bar{j}_b)$, *etc.* Then the two-body matrix elements in the oscillator basis are of the form $\langle cd; J | V | ab; J \rangle$, and we wish to obtain transformed matrix elements $\langle \bar{c} \bar{d}; J | V | \bar{a} \bar{b}; J \rangle$. The basic ingredient is the transformation of single-particle states,

$$|\bar{a}\rangle = \sum_a \langle a | \bar{a} \rangle |a\rangle. \quad (39)$$

The angular functions Y_{lm} and the coupling with spin to yield j are identical for both bases, so $\langle a | \bar{a} \rangle = \langle R_{n_a l_a} | S_{\bar{n}_a \bar{l}_a} \rangle \delta_{(\bar{l}_a \bar{j}_a)(l_a j_a)}$, and the sum over orbitals a in fact only involves a sum over *radial* quantum numbers n_a . In writing out the overlap $\langle R_{n_a l_a} | S_{\bar{n}_a \bar{l}_a} \rangle$, it is worthwhile to explicitly indicate the different choices of length

⁷ We note, however, that the weakly-convergent two-center expansion methods of Ref. [5] might provide a viable approach for carrying out such a transformation.

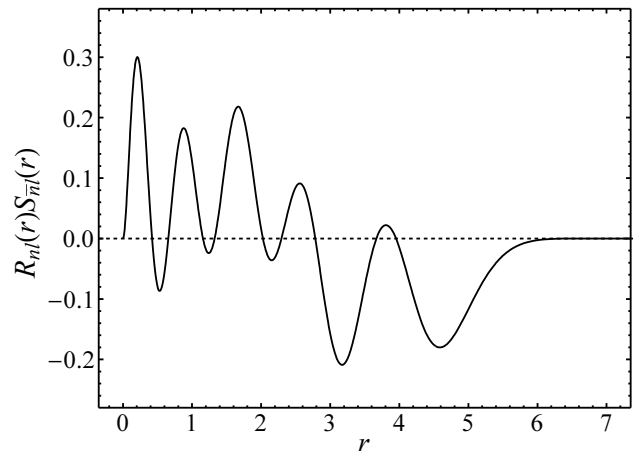


FIG. 2: Integrand $R_{nl}(b_{\text{HO}}; r)S_{\bar{n}l}(b_l; r)$ for the overlap integral (40), taken for a representative case ($l = 0$, $\bar{n} = 5$, and $n = 5$). For this plot, b_l/b_{HO} is given by the prescription (38), and b_{HO} is taken to be unity.

parameter appearing in $R_{nl}(r)$ and $S_{nl}(r)$, for which we adopt the notations $R_{nl}(b; r)$ and $S_{nl}(b; r)$. Then, the overlap is given by the radial integral⁸

$$\langle R_{nl} | S_{\bar{n}l} \rangle = \int_0^\infty dr R_{nl}(b_{\text{HO}}; r) S_{\bar{n}l}(b_l; r). \quad (40)$$

Equivalently, the overlaps may be evaluated in momentum space, as

$$\langle \tilde{R}_{nl} | \tilde{S}_{\bar{n}l} \rangle = \int_0^\infty dk \tilde{R}_{nl}(b_{\text{HO}}; k) \tilde{S}_{\bar{n}l}(b_l; k). \quad (41)$$

When larger values for the radial quantum numbers \bar{n} or n are considered, the integrand appearing in the overlap integral (40) or (41) is highly oscillatory, as illustrated in Fig. 2 — as is to be expected for overlap integrals of functions with large numbers of nodes. Therefore, care must be taken in evaluating the overlap integral through numerical quadrature. Conventional quadrature formulas are found to be slowly-converging and unreliable. However, the zeros of the integrand are easily determined, from the zeros of the generalized Laguerre polynomials or Jacobi polynomials, in terms of which the radial functions are defined, as summarized in Appendix B. Integration can then be carried out in a numerically robust

⁸ The oscillator wavefunctions as defined in (2) are positive at the origin, *i.e.*, as $r \rightarrow 0$. The Coulomb-Sturmian functions as defined in (31) have this property as well. It should be noted that a conventional phase factor $(-)^n$ may be included in the definition of Ψ_{nlm} , so that the functions are instead positive at infinity, *i.e.*, as $r \rightarrow \infty$. If so, this sign must be accounted for in evaluating the transformation bracket (40) for the change of basis. Alternatively, the phase convention for the Coulomb-Sturmian basis may be adjusted analogously.

fashion if the full integration range $[0, \infty)$ is first broken into intervals between successive zeros. Within each interval, the integrand is well-behaved, and conventional numerical quadrature can be carried out reliably. The results may then be summed to give the full integral. It is found that a 32-point Gauss-Legendre quadrature on each interval suffices for present purposes, yielding numerical errors of $\lesssim 10^{-8}$ (and generally much better) for calculations involving radial wavefunctions with $n \lesssim 20$. Integration in the tail region, between the last zero of the integrand and infinity, requires special treatment, since Gauss-Legendre quadrature is only defined on finite intervals. One can map the tail region onto a finite interval by a suitable transformation of integration variable. Alternatively, and most simply, the integration may be truncated at a sufficiently large cutoff r_{\max} , *e.g.*, $r_{\max}/b \approx 50$ is found to suffice in the present calculations.

For proton-neutron matrix elements, the two-body states transform as

$$|\bar{a}\bar{b}; J\rangle_{pn} = \sum_{ab} \langle a|\bar{a}\rangle \langle b|\bar{b}\rangle |ab; J\rangle_{pn}, \quad (42)$$

and the matrix elements consequently transform as

$$\begin{aligned} \langle \bar{c}\bar{d}; J|V|\bar{a}\bar{b}; J\rangle_{pn} \\ = \sum_{abcd} \langle a|\bar{a}\rangle \langle b|\bar{b}\rangle \langle c|\bar{c}\rangle \langle d|\bar{d}\rangle \langle cd; J|V|ab; J\rangle_{pn}. \end{aligned} \quad (43)$$

As noted above for (39), the sums over orbitals a , b , c , and d need only traverse the radial quantum numbers

n_a , n_b , n_c , and n_d , preserving the same angular quantum numbers.

For proton-proton or neutron-neutron matrix elements, normalization considerations related to antisymmetrization must be taken into account in carrying out the transformation. Since different normalization conventions arise in the description of two-particle states, the present conventions are briefly summarized in Appendix C. It is easiest to state the transformation rule if the two-body matrix elements are defined in terms of the *antisymmetrized* (AS) two-particle states $|ab; JM\rangle_{\text{AS}}$ of (C3), which are properly normalized except in the case in which both particles occupy the same orbital. Then, it maybe be seen [*e.g.*, by carrying out a change of basis on the creation operators in (C3) [29]] that we simply have

$$|\bar{a}\bar{b}; J\rangle_{\text{AS}} = \sum_{ab} \langle a|\bar{a}\rangle \langle b|\bar{b}\rangle |ab; J\rangle_{\text{AS}}. \quad (44)$$

Consequently, for the two-body matrix elements,

$$\begin{aligned} \langle \bar{c}\bar{d}; J|V|\bar{a}\bar{b}; J\rangle_{\text{AS}} \\ = \sum_{abcd} \langle a|\bar{a}\rangle \langle b|\bar{b}\rangle \langle c|\bar{c}\rangle \langle d|\bar{d}\rangle \langle cd; J|V|ab; J\rangle_{\text{AS}}. \end{aligned} \quad (45)$$

The corresponding expression for the transformation in terms of the strictly *normalized antisymmetrized* (NAS) states $|ab; JM\rangle_{\text{NAS}}$ of (C5) is less transparent, since the case of identical orbitals must be treated specially within the sum, giving

$$\langle \bar{c}\bar{d}; J|V|\bar{a}\bar{b}; J\rangle_{\text{NAS}} = (1 + \delta_{\bar{a}\bar{b}})^{-1/2} (1 + \delta_{\bar{c}\bar{d}})^{-1/2} \sum_{abcd} (1 + \delta_{ab})^{1/2} (1 + \delta_{cd})^{1/2} \langle a|\bar{a}\rangle \langle b|\bar{b}\rangle \langle c|\bar{c}\rangle \langle d|\bar{d}\rangle \langle cd; J|V|ab; J\rangle_{\text{NAS}}. \quad (46)$$

It is trivial to convert between AS and NAS matrix elements, and thus to use either relation (45) or (46), but it is important to note the distinction.

For actual calculation of the transformed matrix elements, the infinite sums over orbitals appearing in the transformation rule (43) and (45) [or (46)] must be truncated, limited in practice by the available set of oscillator-basis matrix elements. If a shell-based cutoff, *i.e.*, by number of oscillator quanta, is applied to the single-particle space, then $N \leq N_{\text{cut}}$ for the single-particle states, and the sum \sum_{abcd} appearing in (43) and (45) is truncated to $\sum_{N_a, N_b, N_c, N_d \leq N_{\text{cut}}}^{N_a, N_b, N_c, N_d}$. For example, the set of oscillator basis two-body matrix elements required for a transformation with cutoff $N_{\text{cut}} = 13$ (14 shells) consists of 9.2×10^7 proton-neutron two-body matrix elements and 2.3×10^7 proton-proton or neutron-neutron matrix

elements.⁹ The summations (43) or (45) only involve matrix elements sharing the same angular momentum J , parity P , and isospin projection T_z (pn , pp , or nn), and thus in practice the transformation may be carried out separately for each sector of matrix elements, characterized by these quantum numbers. *After* transformation, substantially fewer matrix elements are required for an N_{\max} -truncated many-body calculation in the same number of shells, *e.g.*, for p -shell nuclei, an $N_{\max} = 12$ calcu-

⁹ These are the possible nonzero two-body matrix elements (Appendix C), with single-particle states taken from 14 shells, for an interaction which is parity-conserving but with no further assumptions about isospin (or charge) symmetry. Actual nucleon-nucleon interactions may in fact contain fewer independent matrix elements.

lation involves 14 shells but only 4.1×10^6 proton-neutron two-body matrix elements and 1.0×10^6 proton-proton or neutron-neutron matrix elements, due to the further restriction on N_{tot} .

The accuracy of the resulting two-body matrix elements obtained for the Coulomb-Sturmian basis depends on the inclusion of an adequate number of oscillator shells. The effect of truncation may in general be expected to vary depending on the two-body operator under consideration. In practice, the adequacy of the transformation may be judged by the sensitivity of the final many-body calculation to N_{cut} . Calculations with $N_{\text{cut}} = 9$ (10 shells), $N_{\text{cut}} = 11$ (12 shells), and $N_{\text{cut}} = 13$ (14 shells) are considered in Sec. IV.

Since the change of basis (39) represents a transformation of radial wavefunctions, the underlying approximation in applying a cutoff is that we are effectively representing the Coulomb-Sturmian radial functions in terms of a truncated set of oscillator radial functions, as

$$S_{\bar{n}l}(b_l; r) = \sum_{n \leq N_{\text{cut}}} \langle R_{nl} | S_{\bar{n}l} \rangle R_{nl}(b_{\text{HO}}; r), \quad (47)$$

with $N = 2n + l$, so $n \leq (N_{\text{cut}} - l)/2$. The decomposition of Coulomb-Sturmian functions in terms of oscillator functions, shown as squared amplitudes (probabilities), is given in Fig. 3. Results are shown for the functions previously plotted in Fig. 1(d-f), that is, with $0 \leq n \leq 3$ and for $l = 0, 2$, and 8 , with the length scales of the functions determined according to the prescription (38). While the first two or three CS functions for each value of l are easily expanded in the oscillator basis, the required number of shells is seen to grow rapidly for higher radial quantum numbers. The degree to which the Coulomb-Sturmian radial function is successfully expanded in a truncated set of oscillator radial functions is seen from the dashed curves in Fig. 3, which indicate the accumulated probability $P_n = \sum_{n' \leq n} \langle R_{n'l} | S_{\bar{n}l} \rangle^2$. The set of oscillator radial functions retained in the most generous truncation used in Sec. IV, $N_{\text{cut}} = 13$, can be seen from the vertical dotted line in each panel of Fig. 3.

D. Evaluation of two-body matrix element for separable radial and kinetic operators

If the two-body matrix elements of the entire Hamiltonian are first evaluated in the oscillator basis then transformed to the Coulomb-Sturmian basis, according to the procedure of Sec. III C, it is found (Sec. IV) that the kinetic energy term requires an unacceptably large number of oscillator shells for its expansion. That is, the N_{cut} -dependence of the transformed relative kinetic energy, rather than of the transformed nucleon-nucleon interaction, dominates the cutoff dependence of the many-body calculations.

In this section, we therefore instead consider a scheme which permits the two-body matrix elements of the

center-of-mass and relative components of the r^2 and p^2 operators — R^2 , r_{rel}^2 , P^2 , and p_{rel}^2 — to be evaluated directly in the Coulomb-Sturmian basis. The approach makes use of separability, together with the explicitly known form (35) of the Coulomb-Sturmian radial wavefunction in momentum space. The operators R^2 , r_{rel}^2 , P^2 , and p_{rel}^2 all appear in the NCCI problem. Specifically, p_{rel}^2 appears through the relative kinetic energy operator, r_{rel}^2 through the root-mean-square (RMS) radius observable, and R^2 and P^2 through the center-of-mass oscillator Hamiltonian appearing in the Lawson term. The definitions of and relations among these operators are summarized for reference in Appendix A.

Each of the operators R^2 , r_{rel}^2 , P^2 , and p_{rel}^2 may be decomposed into one-body terms and separable two-body terms. In the following, we let $\mathbf{p} = \hbar \mathbf{k}$ and work with K^2 and k_{rel}^2 instead of P^2 and p_{rel}^2 . Then we have (see Appendix A):

$$\begin{aligned} A^2 R^2 &= \sum_i r_i^2 + \sum'_{ij} \mathbf{r}_i \cdot \mathbf{r}_j \\ A^2 r_{\text{rel}}^2 &= (A-1) \sum_i r_i^2 - \sum'_{ij} \mathbf{r}_i \cdot \mathbf{r}_j \\ K^2 &= \sum_i k_i^2 + \sum'_{ij} \mathbf{k}_i \cdot \mathbf{k}_j \\ k_{\text{rel}}^2 &= (A-1) \sum_i k_i^2 - \sum'_{ij} \mathbf{k}_i \cdot \mathbf{k}_j. \end{aligned} \quad (48)$$

The terms involving \sum_i are manifestly one-body operators, and those involving \sum'_{ij} are manifestly two-body operators. The important property of these expressions (48) for the present approach is that the two-body term in each case — $\sum'_{ij} \mathbf{r}_i \cdot \mathbf{r}_j$ or $\sum'_{ij} \mathbf{p}_i \cdot \mathbf{p}_j$ — has the separable form $\sum'_{ij} \mathbf{T}_i \cdot \mathbf{T}_j$, where \mathbf{T}_k is a spherical tensor (in the present case, rank-1 or vector) operator acting on particle k only. The procedure for calculating two-body matrix elements therefore reduces to the evaluation of radial integrals (either in coordinate space or momentum space, for \mathbf{r}_i or \mathbf{k}_i , respectively), which are then combined using standard angular momentum coupling and recoupling results.

First, let us consider the matrix elements of the one-body terms $\sum_i r_i^2$ and $\sum_i k_i^2$ appearing in (48). For the Coulomb-Sturmian basis, the one-body matrix elements of r^2 and k^2 are

$$\langle b | r^2 | a \rangle = \delta_{l_b l_a} \delta_{j_b j_a} \int_0^\infty dr S_{n_b l_b}(b_{l_b}; r) r^2 S_{n_a l_a}(b_{l_a}; r) \quad (49)$$

and

$$\langle b | k^2 | a \rangle = \delta_{l_b l_a} \delta_{j_b j_a} \int_0^\infty dk \tilde{S}_{n_b l_b}(b_{l_b}; k) k^2 \tilde{S}_{n_a l_a}(b_{l_a}; k). \quad (50)$$

The radial integrals appearing in these expressions may be evaluated by numerical quadrature. Since the integrands are highly oscillatory, the comments and methods of Sec. III C apply to this integration. The integrals

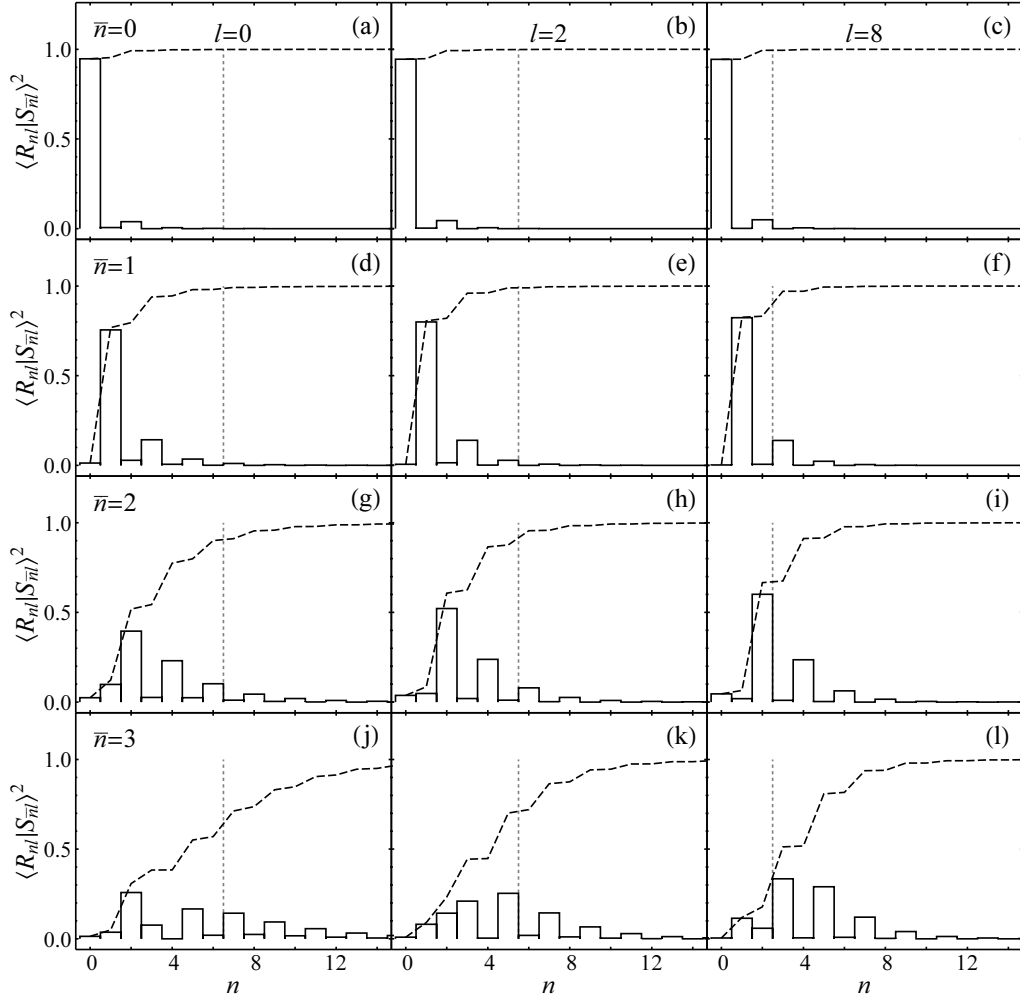


FIG. 3: Probability decomposition of the Coulomb-Sturmian radial functions $S_{\bar{n}l}(b_l; r)$ with respect to the basis of harmonic oscillator radial functions $R_{nl}(b_{HO}; r)$. Results are shown for Coulomb-Sturmian functions with $0 \leq n \leq 3$ (top to bottom) and for $l = 0$ (left), $l = 2$ (center), and $l = 8$ (right), with b_l/b_{HO} given by the node-matching prescription (38). The histogram bars indicate squared amplitudes $\langle R_{nl}(b_{HO}; r) | S_{\bar{n}l}(b_l; r) \rangle^2$ with respect to *individual* oscillator basis functions. The dashed curve indicates accumulated probability, *i.e.*, for *all* oscillator basis functions of lesser or equal n . The vertical dotted line indicates the truncation of the radial basis in effect if the oscillator functions are limited to 14 major shells ($N_{\text{cut}} = 13$), as in the least-truncated calculations of Sec. IV.

are again evaluated piecewise between zeros of the integrands, through Gauss-Legendre quadrature.

Although $\sum_i r_i^2$ and $\sum_i k_i^2$ are one-body operators, they are being considered here as contributions to the two-body operators R^2 , r_{rel}^2 , P^2 , and p_{rel}^2 , through (48), for which *two-body* matrix elements are therefore required as input to the many-body calculation. The appropriate two-body matrix elements are readily obtained from the one-body matrix elements $\langle b | r^2 | a \rangle$ and $\langle b | k^2 | a \rangle$ considered in (49) and (50). In general, corresponding to any one-body operator $U = \sum_i u_i$, we may define a two-body operator V_U via $V_U = \frac{1}{2} \sum_{ij} v_{ij}$, where $v_{ij} = u_i + u_j$. By comparing the sums appearing in the definitions of U and V_U , it may be seen that these operators are identical, except for an A -dependent normalization. Specifically, the

operators are related by

$$U = \frac{1}{A-1} V_U, \quad (51)$$

when acting on the many-body states of an A -particle system.

We therefore consider two-body matrix elements of V_U . For the proton-neutron matrix elements,

$$\langle cd; J | V_U | ab; J \rangle_{pn} = \langle c | U | a \rangle \delta_{db} + \langle d | U | b \rangle \delta_{ca}. \quad (52)$$

For the proton-proton or neutron-neutron matrix elements, the antisymmetrized matrix element may be evaluated by first reexpressing it in terms of unsymmetrized

matrix elements, as

$$\begin{aligned} \langle cd; J|V_U|ab; J\rangle_{AS} &= \langle cd; J|v_{12}|ab; J\rangle \\ &- (-)^{J-j_a-j_b} \langle cd; J|v_{12}|ba; J\rangle, \end{aligned} \quad (53)$$

with v_{ij} as defined above. It follows that

$$\begin{aligned} \langle cd; J|V_U|ab; J\rangle_{AS} &= \langle c|U|a\rangle\delta_{db} + \langle d|U|b\rangle\delta_{ca} \\ &- (-)^{J-j_a-j_b} \langle c|U|b\rangle\delta_{da} - (-)^{J-j_a-j_b} \langle d|U|a\rangle\delta_{cb}. \end{aligned} \quad (54)$$

Thus, the matrix elements of interest for the one-body terms appearing in (48) are obtained by setting $U = r^2$ or k^2 and using one-body matrix elements (49) or (50), respectively, in (52) and (54).

Now let us consider the matrix elements of the two-body terms $\frac{1}{2}\sum'_{ij}\mathbf{r}_i\cdot\mathbf{r}_j$ and $\frac{1}{2}\sum'_{ij}\mathbf{k}_i\cdot\mathbf{k}_j$ appearing in (48). We include a factor of 1/2 in these expressions to bring them into the standard form for two-body operators, namely, $V = \frac{1}{2}\sum'_{ij}v_{ij}$, with $v_{ij} = v_{ji}$. The operator defined by the sum, in either case, is of the separable form $V_{\mathbf{T}_1\cdot\mathbf{T}_2} = \frac{1}{2}\sum'_{ij}\mathbf{T}_i\cdot\mathbf{T}_j$, where \mathbf{T}_i is a vector operator acting on particle i . Since the summand is a spherical tensor product of operators acting on two different subsystems (namely, particles i and j), it is possible to evaluate the matrix elements by Racah's reduction formula [30]. For the proton-neutron matrix elements,

$$\begin{aligned} \langle cd; J|\mathbf{T}_1\cdot\mathbf{T}_2|ab; J\rangle_{pn} \\ = (-)^{j_d+j_a+J} \left\{ \begin{matrix} j_c & j_d & J \\ j_b & j_a & 1 \end{matrix} \right\} \langle c\|\mathbf{T}\|a\rangle\langle d\|\mathbf{T}\|b\rangle. \end{aligned} \quad (55)$$

For the proton-proton and neutron-neutron matrix elements, it is important to note that Racah's reduction formula applies to matrix elements between ordinary, unsymmetrized product states of distinguishable subsystems. Thus, the two-body matrix element between *antisymmetrized* states of two like nucleons must first be expanded by (C3) in terms of unsymmetrized matrix elements, as

$$\begin{aligned} \langle cd; J|V_{\mathbf{T}_1\cdot\mathbf{T}_2}|ab; J\rangle_{AS} &= \langle cd; J|\mathbf{T}_1\cdot\mathbf{T}_2|ab; J\rangle \\ &- (-)^{J-j_a-j_b} \langle cd; J|\mathbf{T}_1\cdot\mathbf{T}_2|ba; J\rangle. \end{aligned} \quad (56)$$

Then, each of the two terms may be evaluated separately through Racah's reduction formula, much as in (55), giving

$$\begin{aligned} \langle cd; J|\mathbf{T}_1\cdot\mathbf{T}_2|ab; J\rangle \\ = (-)^{j_d+j_a+J} \left\{ \begin{matrix} j_c & j_d & J \\ j_b & j_a & 1 \end{matrix} \right\} \langle c\|\mathbf{T}\|a\rangle\langle d\|\mathbf{T}\|b\rangle \end{aligned} \quad (57)$$

for the first term, and similarly with $b \leftrightarrow a$ for the second term.

The one-body reduced matrix elements $\langle b\|\mathbf{T}\|a\rangle$ appearing in (55) or (57) are expressed in terms of radial integrals, using the general relation $x_m = \sqrt{4\pi/3}xY_{1m}(\hat{\mathbf{x}})$ for the spherical components of a coordinate vector \mathbf{x} in terms of Y_1 [24], as

$$\begin{aligned} \langle b\|\mathbf{r}\|a\rangle &= \left(\frac{4\pi}{3}\right)^{1/2} \\ &\times \left[\int_0^\infty dr S_{n_b l_b}(b_{l_b}; r) r S_{n_a l_a}(b_{l_a}; r) \right] \\ &\times \langle l_b j_b \| Y_1 \| l_a j_a \rangle \end{aligned} \quad (58)$$

and

$$\begin{aligned} \langle b\|\mathbf{k}\|a\rangle &= (-)^{(l_b-l_a-1)/2} \left(\frac{4\pi}{3}\right)^{1/2} \\ &\times \left[\int_0^\infty dk \tilde{S}_{n_b l_b}(b_{l_b}; k) k \tilde{S}_{n_a l_a}(b_{l_a}; k) \right] \\ &\times \langle l_b j_b \| Y_1 \| l_a j_a \rangle. \end{aligned} \quad (59)$$

Numerical evaluation of these radial integrals is again subject to the considerations for oscillatory integrands discussed in Sec. III C. The angular factor appearing in (58) and (59) is given by [24]

$$\langle l_b j_b \| Y_1 \| l_a j_a \rangle = \left(\frac{3}{4\pi}\right)^{1/2} (-)^{j_b-j_a+1} (j_a \tfrac{1}{2} 10 | j_b \tfrac{1}{2}) \pi(l_a 1 l_b), \quad (60)$$

where $\pi(l_1 l_2 \dots) \equiv \frac{1}{2}[1 + (-)^{l_1+l_2+\dots}]$. The factor $\pi(l_a 1 l_b)$ enforces the parity selection rule for Y_1 , namely, $l_b - l_a$ odd. Since the angular momentum triangle inequality also applies, the radial matrix elements $\langle b\|\mathbf{r}\|a\rangle$ or $\langle b\|\mathbf{k}\|a\rangle$ need only be evaluated for pairs of orbitals for which $l_b = l_a \pm 1$. The phase factor $(-)^{(l_b-l_a-1)/2}$ in (59) arises from the phase factor $(-i)^l$ in the definition (7) of the momentum-space radial wavefunction, after simplifications are carried out making use of the constraints on l -values imposed by the angular factor (60).

To summarize, the two-body matrix elements of R^2 , r_{rel}^2 , K^2 , or k_{rel}^2 are evaluated by calculating the one body contributions according to (52) or (54) and combining these with the matrix elements of the two-body contribution, calculated according to (55) or (56), via the operator relations (48). Collecting the various contributions and normalization factors, we have

$$\begin{aligned}
\langle cd; J | A^2 R^2 | ab; J \rangle &= \frac{1}{A-1} \langle cd; J | V_{r^2} | ab; J \rangle + 2 \langle cd; J | V_{\mathbf{r}_1 \cdot \mathbf{r}_2} | ab; J \rangle \\
\langle cd; J | A^2 r_{\text{rel}}^2 | ab; J \rangle &= \langle cd; J | V_{r^2} | ab; J \rangle - 2 \langle cd; J | V_{\mathbf{r}_1 \cdot \mathbf{r}_2} | ab; J \rangle \\
\langle cd; J | K^2 | ab; J \rangle &= \frac{1}{A-1} \langle cd; J | V_{k^2} | ab; J \rangle + 2 \langle cd; J | V_{\mathbf{k}_1 \cdot \mathbf{k}_2} | ab; J \rangle \\
\langle cd; J | k_{\text{rel}}^2 | ab; J \rangle &= \langle cd; J | V_{k^2} | ab; J \rangle - 2 \langle cd; J | V_{\mathbf{k}_1 \cdot \mathbf{k}_2} | ab; J \rangle.
\end{aligned} \tag{61}$$

Further practical aspects of evaluating these matrix elements are considered in Appendix D.

Although the separable method described here for evaluating two-body matrix elements of R^2 , r_{rel}^2 , K^2 , and k_{rel}^2 has been presented in the context of the Coulomb-Sturmian basis, this approach is applicable to a general radial basis, so long as both the coordinate-space and momentum-space radial wavefunction can be accurately evaluated and integrated. The only basis dependence lies in evaluating the radial integrals (49), (50), (58), and (59). For instance, the separable method can be used with the oscillator basis, applied to the radial functions $R_{nl}(r)$ of (4) and $\tilde{R}_{nl}(k)$ of (9), in lieu of Moshinsky transformation.¹⁰

IV. COULOMB-STURMIAN CALCULATIONS FOR ${}^6\text{Li}$

A. Overview

As a basic illustration of the use of the Coulomb-Sturmian basis for NCCI calculations, we consider the nucleus ${}^6\text{Li}$. The code MFDn [31–33] is used for the many-body calculations, taking as its input Hamiltonian two-body matrix elements obtained according to the procedures developed in Secs. III C and III D. Calculations are carried out with respect to a proton-neutron M -scheme basis.

The question arises as to how to truncate a many-body basis built from Coulomb-Sturmian functions. For the present calculation, we *formally* carry over the N_{max} truncation scheme to the Coulomb-Sturmian basis. That is, for each Coulomb-Sturmian single-particle state, we define $N = 2n + l$. Then, as for the oscillator basis, we label the many-body states by the sum $N_{\text{tot}} = \sum_i N_i$ and apply the N_{max} truncation as defined in (20). Since n is now the radial quantum number for the Coulomb-Sturmian functions, the label N no longer has any direct

significance in terms of oscillator quanta. Furthermore, when applied to the Coulomb-Sturmian basis, the N_{max} truncation does *not* imply the exact separation properties described in Sec. II C, nor can it any longer be interpreted as an “energy” truncation, with respect to some noninteracting Hamiltonian. Nonetheless, as one of many conceivable truncation schemes, the N_{max} scheme provides a reasonable starting point for further exploration, and it is particularly convenient for use with existing NCCI many-body codes. Furthermore, using an N_{max} truncation facilitates comparison of convergence rates obtained using the oscillator and Coulomb-Sturmian bases, since the dimensions of the many-body spaces are then the same in both cases.

The result for any given observable has a twofold dependence on the basis used: on the truncation and on the length parameter. In the existing literature on the NCCI approach with the oscillator basis, the oscillator length b for the basis is commonly not stated directly, but rather the oscillator energy $\hbar\Omega$ is given, in terms of which we recall $b = [\hbar/(m_N\Omega)]^{1/2}$. For consistency, we therefore adopt the same convention for the Coulomb-Sturmian basis. However, it must be borne in mind that the $\hbar\Omega$ value quoted for the Coulomb-Sturmian basis is simply the $\hbar\Omega$ of the *reference* oscillator length b_{HO} , from which the actual l -dependent length parameters b_l are derived by the node-matching prescription of Sec. III B. It therefore has no *direct* significance as an energy scale for the problem. When comparing calculations in the harmonic oscillator basis and in the Coulomb-Sturmian basis, the relationship of $\hbar\Omega$ values between the two calculations should therefore also not be viewed as one of strict physical equivalence, *e.g.*, it is not necessarily most appropriate to compare an $\hbar\Omega = 20$ MeV oscillator basis calculation with an $\hbar\Omega = 20$ MeV Coulomb-Sturmian basis calculation. Rather, a set of calculations for each basis, spanning a range of $\hbar\Omega$ values, should be considered, and best convergence may be obtained for different $\hbar\Omega$ values in each of the two bases. However, for either basis, the same proportionality $b \propto (\hbar\Omega)^{-1/2}$ holds, *e.g.*, a doubling in $\hbar\Omega$ corresponds to a factor of $\sqrt{2}$ contraction of the length scale.

The present ${}^6\text{Li}$ calculations are carried out for the JISP16 interaction [34], which is a two-body interaction derived from neutron-proton scattering data and adjusted via a phase-shift equivalent transformation to describe light nuclei without explicit three-body interac-

¹⁰ In fact, the separable method has been used to evaluate the matrix elements of the T_{rel} , $N_{\text{c.m.}}$, and r_{rel}^2 operators for the oscillator-basis NCCI calculations shown in Sec. IV. Comparison against the results obtained with existing Moshinsky-based oscillator-basis calculations provides a vital means of validating the present computational framework for general bases.

tions. All calculations shown here are for the positive-parity space, spanned by states with even values $N_{\text{tot}} = N_0, N_0 + 2, \dots, N_0 + N_{\text{max}}$. Although isospin is not strictly conserved by the Hamiltonian, due to the Coulomb interaction, the isospin T is essentially a good quantum number for the states in the present calculations. Therefore, for simplicity, we restrict attention to the $T = 0$ spectrum. Calculations are carried out in several truncated spaces with $N_{\text{max}} \leq 10$, to provide an initial investigation into convergence.

The nucleus ${}^6\text{Li}$ provides a useful case for benchmarking, since calculations with comparatively large values of N_{max} are feasible with the most-powerful presently-available computational resources, and detailed extrapolation studies have recently been carried using the conventional oscillator basis in such large spaces, specifically, $N_{\text{max}} \leq 16$, with the same interaction as used here [35]. These results provide estimates for the true values of observables, against which the present Coulomb-Sturmian calculations in smaller spaces can be compared.

B. Energies

We begin by comparing the ground state energy obtained in NCCI calculations with the conventional oscillator basis and with the Coulomb-Sturmian basis. The calculated energies of the 1^+ ground state of ${}^6\text{Li}$ are shown for the oscillator basis in Fig. 4(a) and for the Coulomb-Sturmian basis in Fig. 4(b). In each case, the calculations span a range of $\hbar\Omega$ values from 10 MeV to 40 MeV and are carried out for $N_{\text{max}} = 4, 6, 8$, and 10. These N_{max} values correspond to the highest to lowest curves, respectively, in the figure. The bare Hamiltonian has been used, without renormalization to the finite space, so the variational principle is in effect, and energies (for the lowest state with each set of conserved quantum numbers) approach the full-space value monotonically from above with increasing N_{max} .

The goal is not for any single NCCI calculation to actually *reach* a converged value, but rather to obtain the most reliable *extrapolation* from a series of NCCI calculations, to the converged value which would be obtained in the full, untruncated space for the many-body problem [13–15]. It is thus first necessary to examine the dependence of the results on the basis parameters $\hbar\Omega$ and N_{max} as just described. Extrapolation schemes are still largely empirical in their justification, and different prescriptions, varying in their details, might be used. However, for energies, at least, the basic procedure explored in, *e.g.*, Refs. [13, 14, 36], consists of an exponential extrapolation. The no-core full configuration (NCFC) approach [14], in particular, is based on exponential extrapolations of results of calculations obtained with an unrenormalized interaction appropriate to the infinite, untruncated space, so that energies approach the full-space values monotonically, as noted above. One first finds the variational minimum with respect to $\hbar\Omega$, for the highest

available N_{max} -truncated space. Then one extrapolates with respect to N_{max} , at this $\hbar\Omega$, to the full-space result ($N_{\text{max}} \rightarrow \infty$) by assuming an exponential approach to the asymptotic value E_∞ ,

$$E(N_{\text{max}}) = E_\infty + ae^{-cN_{\text{max}}}, \quad (62)$$

where E_∞ , a , and c are taken as parameters.

As the baseline for comparison, the calculations of the ground state energy with the oscillator basis are shown in Fig. 4(a). The variational minimum with respect to $\hbar\Omega$ occurs at ~ 20 MeV, for $N_{\text{max}} = 10$, moving gradually lower with increasing N_{max} . For each value of $\hbar\Omega$ at which calculations have been carried out, an exponential extrapolation of the $N_{\text{max}} = 4$ –10 calculations is shown (indicated by a cross). The best estimate of the ground state energy from Ref. [35], $E = -31.49(3)$ MeV, is indicated by the dashed horizontal line. The extrapolated values pass through this estimate at $\hbar\Omega \approx 20$ MeV, that is, roughly the location of the variational minimum.

The calculations of the ground state energy with the Coulomb-Sturmian basis are shown in Fig. 4(b). The variational minimum with respect to $\hbar\Omega$ occurs at ~ 30 MeV, for $N_{\text{max}} = 10$, and moves *higher* with increasing N_{max} . Notice that at each N_{max} the variational minimum energy obtained with the Coulomb-Sturmian basis is substantially higher than that obtained with the oscillator basis (by ~ 2 MeV for $N_{\text{max}} = 10$). However, the energies obtained with the Coulomb-Sturmian basis are also falling significantly more rapidly with increasing N_{max} . (In general, a higher *starting* energy for the convergence, at low N_{max} , need not imply a lower *rate* of convergence.) Therefore, let us compare the exponential fit parameters [see (62)] near the variational minimum. For the oscillator basis at $\hbar\Omega = 20$ MeV, the convergence rate is $c \approx 0.35$, with an extrapolated ground state energy of -31.3 MeV. For the Coulomb-Sturmian basis at $\hbar\Omega = 30$ MeV, the convergence rate is comparable, albeit marginally lower, at $c \approx 0.29$, with an extrapolated ground state energy which is also comparable, at -31.2 MeV. Interestingly, the extrapolations for the Coulomb-Sturmian basis have a qualitatively different dependence on $\hbar\Omega$ than those for the oscillator basis. Rather than varying monotonically (increasing with increasing $\hbar\Omega$), they have a minimum, at an $\hbar\Omega$ approximately equal to that of the variational minimum.

The one significant numerical approximation which is entailed in setting up the Coulomb-Sturmian calculations, as discussed in Sec. III C, is in the transformation of the two-body matrix elements of the nucleon-nucleon interaction from the oscillator basis to the Coulomb-Sturmian basis. The transformation is necessarily carried out in a truncated oscillator basis. It is therefore imperative to establish the numerical stability of the results with respect to the shell truncation N_{cut} in the sum over oscillator states. Calculations based on two-body matrix elements obtained with $N_{\text{cut}} = 9$ (10 shells), $N_{\text{cut}} = 11$ (12 shells), and $N_{\text{cut}} = 13$ (14 shells) are overlaid in Fig. 4(b), as well as in all subsequent plots of Coulomb-

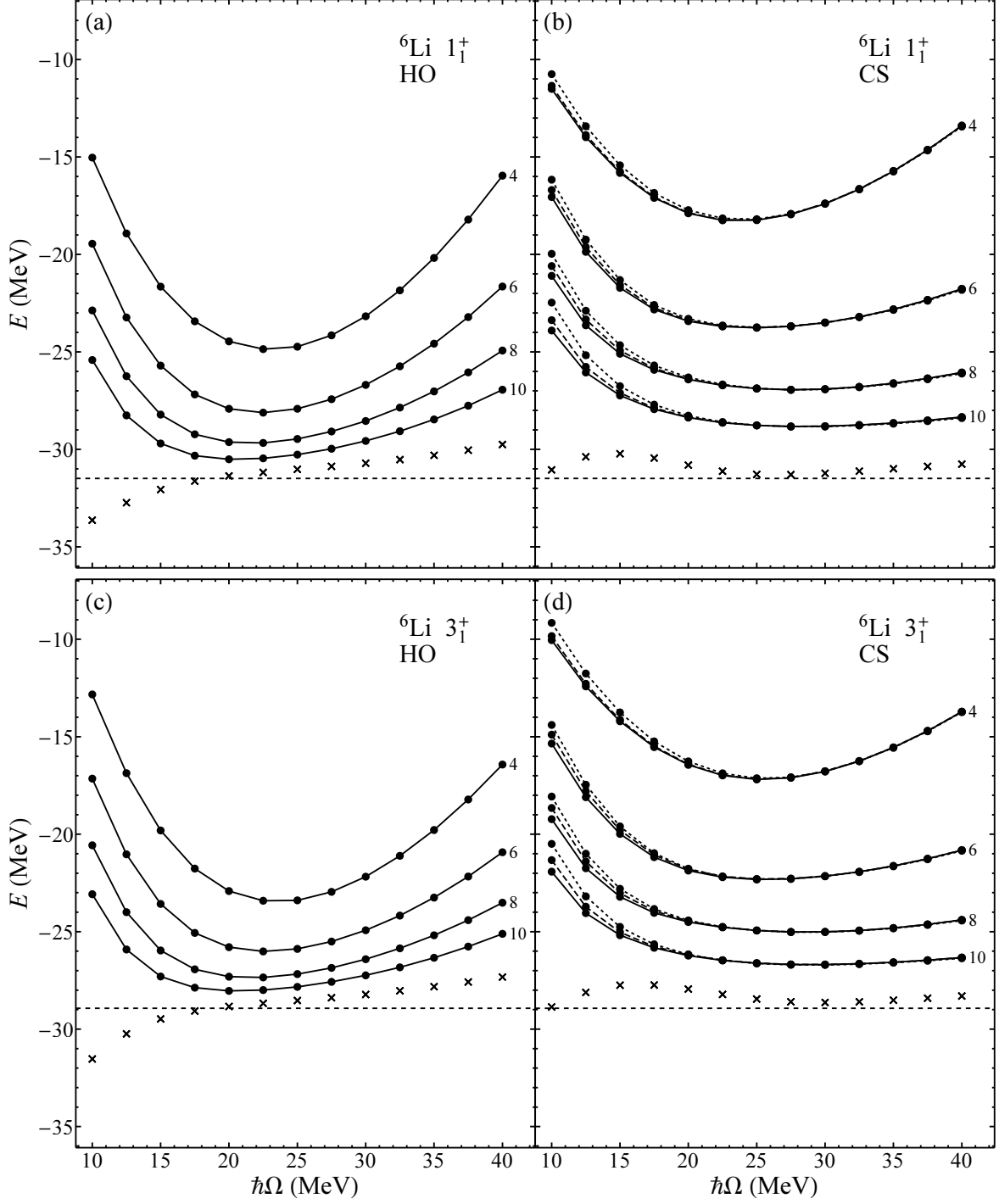


FIG. 4: The ${}^6\text{Li}$ 1^+ ground state energy (top) and 3^+ excited state energy (bottom), calculated using the conventional harmonic oscillator basis (left) and the Coulomb-Sturmian basis (right). Calculated energies are plotted as a function of the basis $\hbar\Omega$ parameter, for $N_{\text{max}} = 4, 6, 8$, and 10 (successive curves, as labeled). For the Coulomb-Sturmian basis, calculations are shown variously for truncations $N_{\text{cut}} = 9$ (dotted curves), $N_{\text{cut}} = 11$ (dashed curves), and $N_{\text{cut}} = 13$ (solid curves) in the change-of-basis transformation of two-body matrix elements. Exponentially extrapolated values (based on the $N_{\text{cut}} = 13$ calculations in the case of the Coulomb-Sturmian basis) are indicated by crosses (\times). The best extrapolated values from the large-basis calculations of Ref. [35] are shown as horizontal dashed lines.

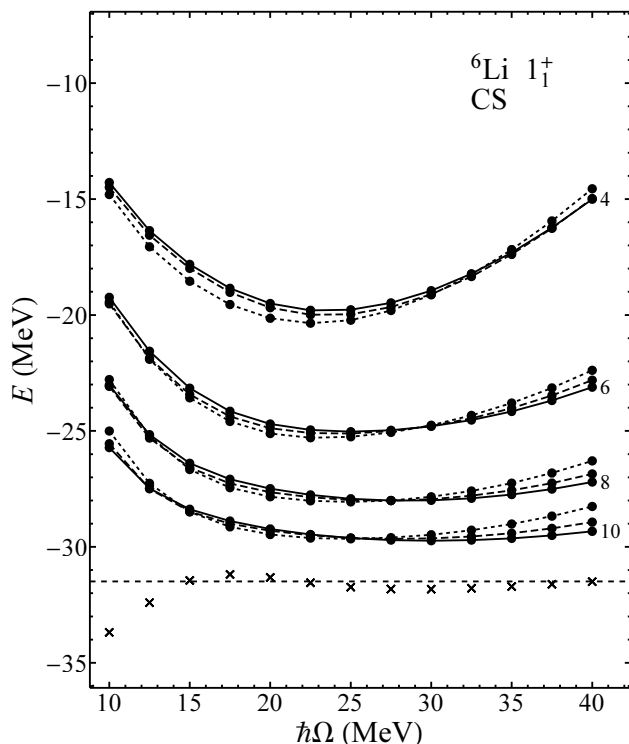


FIG. 5: The ${}^6\text{Li } 1^+$ ground state energy, calculated using the Coulomb-Sturmian basis, but *without* making use of the separable method of Sec. III D for the two-body matrix elements of the T_{rel} operator, for comparison with Fig. 4(b). That is, the entire Hamiltonian, including T_{rel} , is transformed from the oscillator basis following the approach of Sec. III C. See the caption to Fig. 4 for further explanation of curves and symbols.

Sturmian calculations. Calculations of the ground state energy for $\hbar\Omega \gtrsim 20$ MeV are highly stable with respect to this cutoff, in the present calculations. This range safely covers the variational minimum. However, the calculations are not stable with respect to this cutoff for $\hbar\Omega \lesssim 20$ MeV, and higher cutoffs would therefore be required for accurate results at these $\hbar\Omega$ values. The instability with respect to oscillator basis cutoff appears to increase with increasing N_{max} . Such a dependence is reasonable, since higher- N_{max} calculations increasingly probe higher- n Coulomb-Sturmian single-particle basis functions, which in turn require a higher N_{cut} for accurate expansion in an oscillator basis, as illustrated in Fig. 3.

For the calculations shown in Fig. 4, the kinetic energy matrix elements have been calculated by the separable method of Sec. III D. It is interesting at this point to investigate how essential it is to use the separable approach, rather than simply transforming the kinetic energy matrix elements from the oscillator basis. For comparison, we therefore repeat the calculations for the ground state energy in the Coulomb-Sturmian basis, but transforming the two-body matrix elements of the entire Hamiltonian

from the oscillator basis, yielding the results shown in Fig. 5. It is seen that, without the separable calculation, the results are unstable with respect to N_{cut} throughout the entire range of $\hbar\Omega$ values, including the vicinity of the variational minimum. Thus, the separable method plays a major role in obtaining numerically accurate calculations. It would otherwise be necessary to start from oscillator two-body matrix elements in a significantly larger number of oscillator shells, possibly prohibitively so.

Calculations for the energy of the 3^+ first excited state for the oscillator basis are shown in Fig. 4(c) and for the Coulomb-Sturmian basis in Fig. 4(d). The results are very similar in nature to those for the ground state, so little additional discussion is required. The best extrapolation from Ref. [35] places this state at 2.56(2) MeV excitation energy, corresponding to $E \approx -28.93$ MeV. For the oscillator basis at $\hbar\Omega = 20$ MeV, the convergence rate is $c \approx 0.34$, with an extrapolated ground state energy of -28.8 MeV. For the Coulomb-Sturmian basis at $\hbar\Omega = 30$ MeV, the convergence rate is again marginally lower, at $c \approx 0.30$, with an extrapolated energy of -28.6 MeV, apparently erring on the high side relative to Ref. [35].

From these exploratory calculations for ${}^6\text{Li}$, it would appear that convergence properties for energies with the Coulomb-Sturmian basis are comparable, *i.e.*, not markedly inferior, to those of the oscillator basis, with some qualitative differences in the $\hbar\Omega$ dependence. We note that these exploratory results have not yet probed the variational freedoms available with the Coulomb-Sturmian basis, both in the choice of length parameters (Sec. III B) and in truncation schemes, as described above. The convergence rate alone does not provide conclusive information on the robustness which can be expected from large- N_{max} extrapolation or on the best extrapolation procedure. Some questions regarding extrapolation may be elucidated by extending the calculations to higher N_{max} . Furthermore, the rates of convergence of calculations with the oscillator and Coulomb-Sturmian bases will depend on the physical properties of the nucleus (and particular state) under consideration. For instance, the asymptotic properties of the single-particle basis may well play a larger role for halo nuclei or for states involving clusters with significant spatial separation.

C. Root-mean-square radius

The root-mean-square (RMS) radius presents challenges for convergence in NCCI calculations with the conventional oscillator basis [36]. Here we consider the intrinsic, point-nucleon RMS radius for the ground state, defined by $\sqrt{\langle r_{\text{rel}}^2 \rangle}$ (see Appendix A), from which the center-of-mass contribution has been removed by construction. Evaluation of the expectation value $\langle r_{\text{rel}}^2 \rangle$ in a many-body state requires that one first calculate the two-body matrix elements of the r_{rel}^2 operator. These are

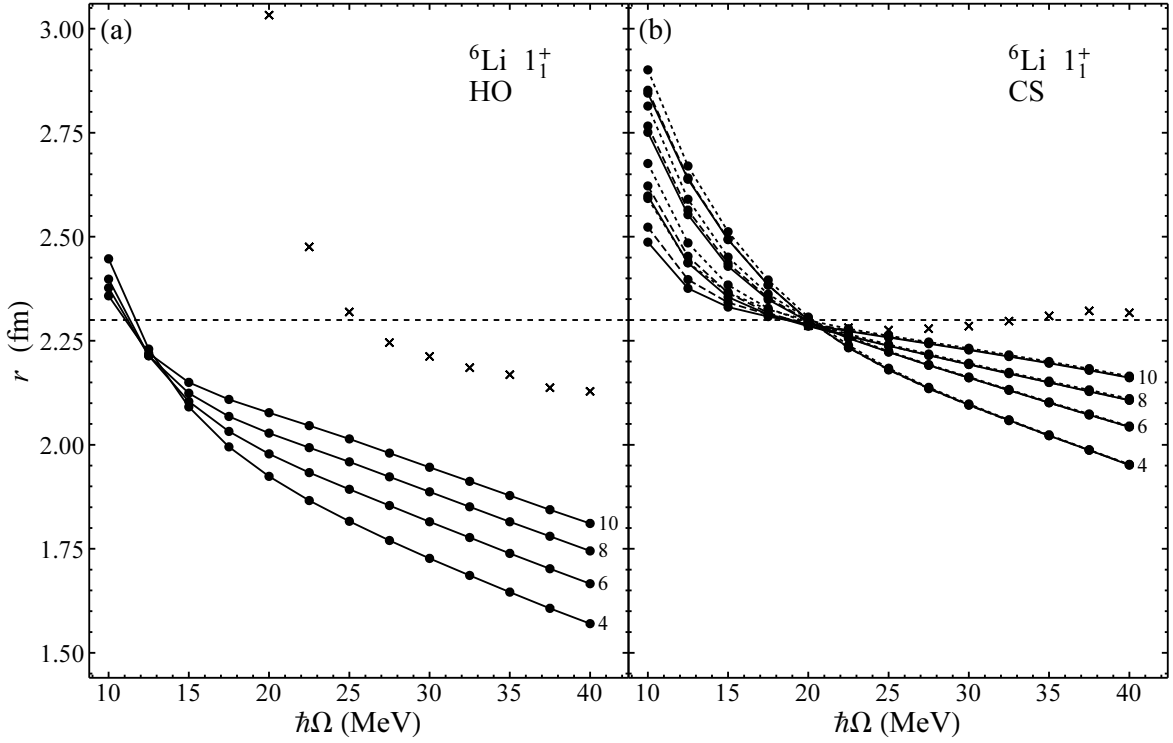


FIG. 6: The ${}^6\text{Li } 1^+$ ground state RMS radius, calculated using the conventional harmonic oscillator basis (left) and the Coulomb-Sturmian basis (right). Calculated energies are plotted as a function of the basis $\hbar\Omega$ parameter, for $N_{\text{max}} = 4, 6, 8$, and 10 (successive curves, as labeled). For the Coulomb-Sturmian basis, calculations are shown variously for truncations $N_{\text{cut}} = 9$ (dotted curves), $N_{\text{cut}} = 11$ (dashed curves), and $N_{\text{cut}} = 13$ (solid curves) in the change-of-basis transformation of two-body matrix elements. Exponentially extrapolated values (based on the $N_{\text{cut}} = 13$ calculations in the case of the Coulomb-Sturmian basis) are indicated by crosses (\times). The best estimated value from the large-basis calculations of Ref. [35] is shown as a horizontal dashed line.

obtained for the Coulomb-Sturmian basis by the separable method of Sec. III D.

The oscillator basis results for the RMS radius in Fig. 6(a) are shown for the same range of calculations ($N_{\text{max}} = 4, 6, 8$, and 10 , with $\hbar\Omega$ values from 10 MeV to 40 MeV) as for the energies in Sec. IV C. (The curves proceed from greatest to least slope with increasing N_{max} in the figure.) Exponential extrapolations to infinite N_{max} are shown as well. The extrapolated values vary strongly with $\hbar\Omega$ and converge very slowly with N_{max} . For instance, taking $\hbar\Omega$ at the variational minimum for the energy, *i.e.*, $\hbar\Omega \approx 20$, the exponential convergence rate for the RMS radius with respect to N_{max} is only $c \approx 0.024$, and the extrapolated radius lies ~ 1 fm above the calculated values. Alternatively, the value at the crossover point of the curves obtained for different N_{max} has also been proposed as an estimate of the full-space value [36]. This crossover occurs at $\hbar\Omega \approx 12$ MeV in the present calculations and lies in the vicinity of 2.2 fm. The best estimate from Ref. [35], similarly obtained from the crossover point, for calculations with $N_{\text{max}} \leq 16$, is ~ 2.3 fm, indicated by the dashed horizontal line in Fig. 6.

Examining the calculations for the RMS radius using the Coulomb-Sturmian basis, as shown in Fig. 6(b), the

gross features are similar. The crossover point for the curves obtained with N_{max} lies at $\hbar\Omega \approx 20$. The value of ~ 2.3 fm is consistent with the estimate of Ref. [35] and ~ 0.1 fm higher than the crossover for the curves obtained with the oscillator basis, for the same N_{max} , in Fig. 6(a). Moreover, it is seen that exponential extrapolation may be a viable approach to estimating the full-space value for the radius. The extrapolated values obtained for $\hbar\Omega \gtrsim 20$ MeV, *i.e.*, above the crossover point, are reasonably insensitive to $\hbar\Omega$ and are consistent with the best estimate from Ref. [35]. For instance, taking $\hbar\Omega \approx 30$, *i.e.*, at the variational minimum, the exponential convergence rate for the RMS radius is $c \approx 0.19$, and the extrapolated radius is ~ 2.28 fm. Results are stable with respect to the shell cutoff in the transformation of matrix elements from the oscillator basis, for $\hbar\Omega \gtrsim 20$ MeV, as observed above for the energies.

It would thus appear that the rate of convergence of the RMS radius obtained with the Coulomb-Sturmian basis is superior to that obtained with the conventional oscillator basis. However, further systematic investigation is required, especially into the stability of extrapolations with increasing N_{max} , before general conclusions may be drawn.

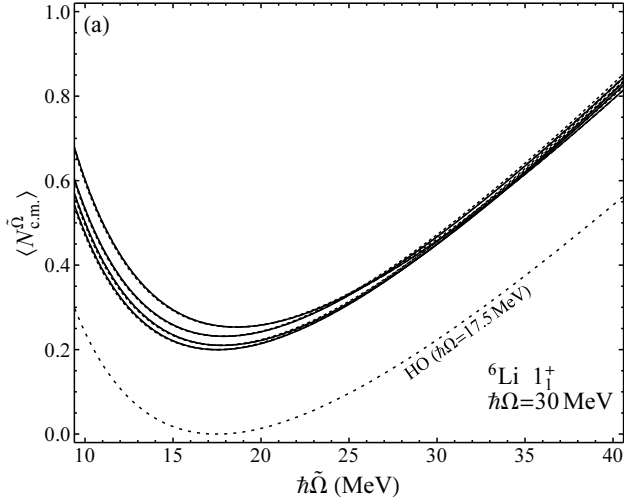


FIG. 7: Expectation value of the number operator $N_{\text{c.m.}}^{\tilde{\Omega}}$ for center-of-mass oscillator quanta, as a function of oscillator energy $\hbar\tilde{\Omega}$. These calculations are for the ${}^6\text{Li } 1^+$ ground state, using the Coulomb-Sturmian basis, with $\hbar\Omega = 30$ MeV. Calculations are shown for $N_{\text{max}} = 4, 6, 8$, and 10 (successive curves, top to bottom), and for truncations $N_{\text{cut}} = 9$ (dotted curves), $N_{\text{cut}} = 11$ (dashed curves), and $N_{\text{cut}} = 13$ (solid curves) in the change-of-basis transformation of two-body matrix elements. The analogous curve expected for a pure harmonic oscillator $0s$ function, with $\hbar\Omega = 17.5$ MeV, is also shown for comparison (dotted curve, labeled).

D. Center-of-mass dynamics

We now focus on the dominant concern in using any basis other than the harmonic oscillator basis with N_{max} truncation for nuclear many-body calculations, namely, incomplete separation of center-of-mass and intrinsic dynamics. There are several aspects to consider: the natural degree of separation arising in calculations using the Coulomb-Sturmian basis, the spurious state spectrum obtained in such calculations, and the extent to which a Lawson term can be used to influence spurious excitations.

The problem of correcting for, or eliminating, spurious contributions for calculations with a general truncated basis is unresolved [37]. Nonetheless, it is still possible that factorized wavefunctions might approximately be obtained in a truncated space. In the full space, factorization is obtained due to the separable Hamiltonian, albeit with degeneracies in the center-of-mass wavefunctions multiplying each intrinsic state (Sec. II B). Therefore, as larger truncated spaces are taken, approaching this full space, the structure of the eigenstates may be expected to converge towards such factorized structure. For instance, a high degree of factorization has been reported for coupled-cluster calculations in light nuclei [38]. Furthermore, introducing a Lawson term to the Hamiltonian, as in (18), may serve to “purify” the eigenstates so that the motion more closely approximates $0s$ center-of-

mass motion, as proposed by Gloeckner and Lawson [20]. This Lawson term also pushes eigenstates dominated by other center-of-mass excitations higher in the spectrum. However, caution must be exercised in such use of the Lawson term, since any improved (or, at least, more oscillator-like) description of center-of-mass motion may be obtained at the expense of the quality with which the intrinsic wavefunction is approximated [39].

A first indication of the degree of separation in the many-body eigenstate is provided by the expectation value of the $N_{\text{c.m.}}$ operator. This operator is defined, for an arbitrary center-of-mass harmonic oscillator energy $\hbar\tilde{\Omega}$, by

$$N_{\text{c.m.}}^{\tilde{\Omega}} \equiv \frac{1}{\hbar\tilde{\Omega}} \left(\frac{P^2}{2Am_N} + \frac{Am_N\tilde{\Omega}^2 R^2}{2} - \frac{3\hbar\tilde{\Omega}}{2} \right), \quad (63)$$

where the tilde serves to distinguish $\hbar\tilde{\Omega}$ from the basis $\hbar\Omega$ parameter. As noted by Hagen *et al.* [38], if separation occurs, as $\psi(\mathbf{r}_i; \boldsymbol{\sigma}_i) = \psi_{\text{c.m.}}(\mathbf{R})\psi_{\text{in}}(\mathbf{r}_{ij}; \boldsymbol{\sigma}_i)$, and if $\psi_{\text{c.m.}}(\mathbf{R})$ happens to be an oscillator $0s$ function, corresponding to some oscillator energy $\hbar\tilde{\Omega}$, then the many-body wavefunction will have $\langle N_{\text{c.m.}}^{\tilde{\Omega}} \rangle = 0$. Evaluation of the expectation value $\langle N_{\text{c.m.}}^{\tilde{\Omega}} \rangle$ requires that one first calculate the two-body matrix elements of P^2 and R^2 , and thence of $N_{\text{c.m.}}^{\tilde{\Omega}}$. These are readily obtained for the Coulomb-Sturmian basis by the separable method of Sec. III D, so evaluation is straightforward.

The expectation value $\langle N_{\text{c.m.}}^{\tilde{\Omega}} \rangle$ is shown as a function of $\hbar\tilde{\Omega}$ for the ${}^6\text{Li } 1^+$ ground state in Fig. 7, for the Coulomb-Sturmian basis calculation with basis $\hbar\Omega = 30$ MeV and no Lawson term. The minimum value of $\langle N_{\text{c.m.}}^{\tilde{\Omega}} \rangle$ is obtained at $\hbar\tilde{\Omega} \approx 17.5$ MeV, shifting gradually towards lower $\hbar\tilde{\Omega}$, which corresponds to larger center-of-mass oscillator length $b_{\text{c.m.}} = [\hbar/(Am_N\Omega)]^{1/2}$, with increasing N_{max} . (The location of the minimum also depends modestly upon the choice of basis $\hbar\Omega$ for the calculation, increasing with $\hbar\Omega$.) The minimum value of $\langle N_{\text{c.m.}}^{\tilde{\Omega}} \rangle$ decreases with increasing N_{max} , but it appears to be converging towards a *nonzero* value of ~ 0.2 . The fact that $\langle N_{\text{c.m.}}^{\tilde{\Omega}} \rangle$ values significantly less than unity are obtained in the calculations indicates that a $0s$ oscillator function dominates the center-of-mass motion, and that an approximate separation of center-of-mass and intrinsic functions is spontaneously arising. However, the nonzero limit indicates that, as the full space is approached, the separated center-of-mass function is *not* strictly taking the form of a $0s$ oscillator function. For comparison, the dependence of $\langle N_{\text{c.m.}}^{\tilde{\Omega}} \rangle$ on $\hbar\tilde{\Omega}$ which would be obtained for a pure oscillator $0s$ function with $\hbar\Omega = 17.5$ MeV, given by $\langle N_{\text{c.m.}}^{\tilde{\Omega}} \rangle = \frac{3}{4}(\Omega/\tilde{\Omega} + \tilde{\Omega}/\Omega - 2)$, is also shown in Fig. 7.

In interpreting these results, it must be stressed that calculating $\langle N_{\text{c.m.}}^{\tilde{\Omega}} \rangle$ for an eigenstate provides only a lower limit on the degree of factorization. That is, a nonzero $\langle N_{\text{c.m.}}^{\tilde{\Omega}} \rangle$ does not preclude factorization but can simply indicate that the factorized center-of-mass wavefunction is not of $0s$ oscillator type. Extracting the true degree of

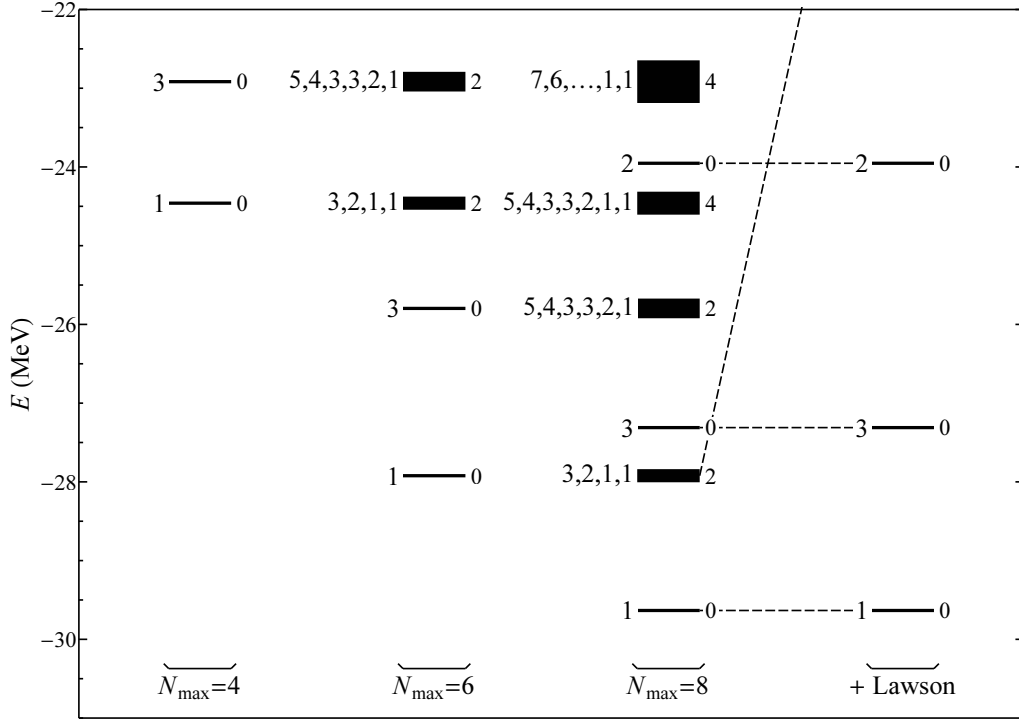


FIG. 8: Level spectrum for ${}^6\text{Li}$, including spurious states, calculated using the conventional harmonic oscillator basis. Calculations (left to right) are for $N_{\text{max}} = 4, 6$, and 8 , and then shown again for $N_{\text{max}} = 8$ with addition of a Lawson term, of sufficient strength to shift the spurious states above the energy range displayed in this plot. For each level, the angular momentum J is indicated at left, and $\langle N_{\text{c.m.}} \rangle$ is indicated at right. For degenerate multiplets of spurious states, the thickness of the line is proportional to the number of states. These calculation are for $\hbar\Omega = 20$ MeV.

factorization is more challenging. To do so likely requires some form of explicit transformation to center-of-mass and relative coordinates. For instance, an expansion $\psi = \sum_i s_i \psi_{\text{c.m.}}^{(i)} \psi_{\text{in}}^{(i)}$ may then be obtained through a singular value decomposition as proposed in Ref. [38].

Since factorization arises in the full space, the effects of convergence of the center-of-mass dynamics were already implicitly included in the extrapolations to the full-space values of the observables of interest, as explored in Secs. IV B and IV C. However, for this extrapolation to be possible, it is necessary that states involving spurious excitations of the center-of-mass function can be disentangled and removed from the low-lying spectrum. This becomes an increasing concern with increasing N_{max} , as we shall now see from examining the spurious state spectrum.

It is helpful to first consider the eigenvalue spectrum, including spurious states, obtained in calculations with an N_{max} -truncated oscillator basis. This is illustrated for ${}^6\text{Li}$ in Fig. 8, for $N_{\text{max}} = 4, 6$, and 8 , with $\hbar\Omega = 20$ MeV. The eigenvalue of $N_{\text{c.m.}}$ is indicated to the right of each level in this figure. For instance, at $N_{\text{max}} = 4$, where the two lowest states in the spectrum are shown, these states have $N_{\text{c.m.}} = 0$ and are thus nonspurious, corresponding to the intrinsic 1^+ ground state and 3^+ first excited state, with $0s$ center-of-mass motion.

Let us examine the evolution of the spectrum in Fig. 8 with increasing N_{max} , bearing in mind the direct sum structure (21) of the N_{max} -truncated space. Moving from $N_{\text{max}} = 4$ to $N_{\text{max}} = 6$, the two additional oscillator quanta introduced to the system may go towards converging the intrinsic states. This yields the new 1^+ ground state and 3^+ excited state at lower energies in the $N_{\text{max}} = 6$ calculation (in the $\mathcal{H}_{\text{c.m.}}^0 \otimes \mathcal{H}_{\text{in}}^6$ subspace). Alternatively, the two additional quanta may go into center-of-mass excitation, yielding spurious states (in the $\mathcal{H}_{\text{c.m.}}^2 \otimes \mathcal{H}_{\text{in}}^4$ subspace). Since the center-of-mass excitation gives no contribution to the energy, under the *intrinsic* Hamiltonian we are using, the resulting spurious states are degenerate with the nonspurious states obtained at $N_{\text{max}} = 4$ (in the $\mathcal{H}_{\text{c.m.}}^0 \otimes \mathcal{H}_{\text{in}}^4$ subspace). Then, moving to $N_{\text{max}} = 8$, new $N_{\text{c.m.}} = 2$ spurious states appear degenerate with the $N_{\text{max}} = 6$ nonspurious states, new $N_{\text{c.m.}} = 4$ spurious states appear degenerate with the $N_{\text{c.m.}} = 2$ spurious states from $N_{\text{max}} = 6$, etc.

To ascertain the angular momenta expected for the spurious states, we note that angular momentum eigenstates of the full eigenproblem are obtained from those of the intrinsic eigenproblem via angular momentum coupling as $\psi^{(J)} = [\psi_{\text{c.m.}}^{(l_{\text{c.m.}})} \times \psi_{\text{in}}^{(J_{\text{in}})}]^{(J)}$. Thus, the angular momenta expected for the spurious states follow by the triangle inequality for addition of the center-of-mass

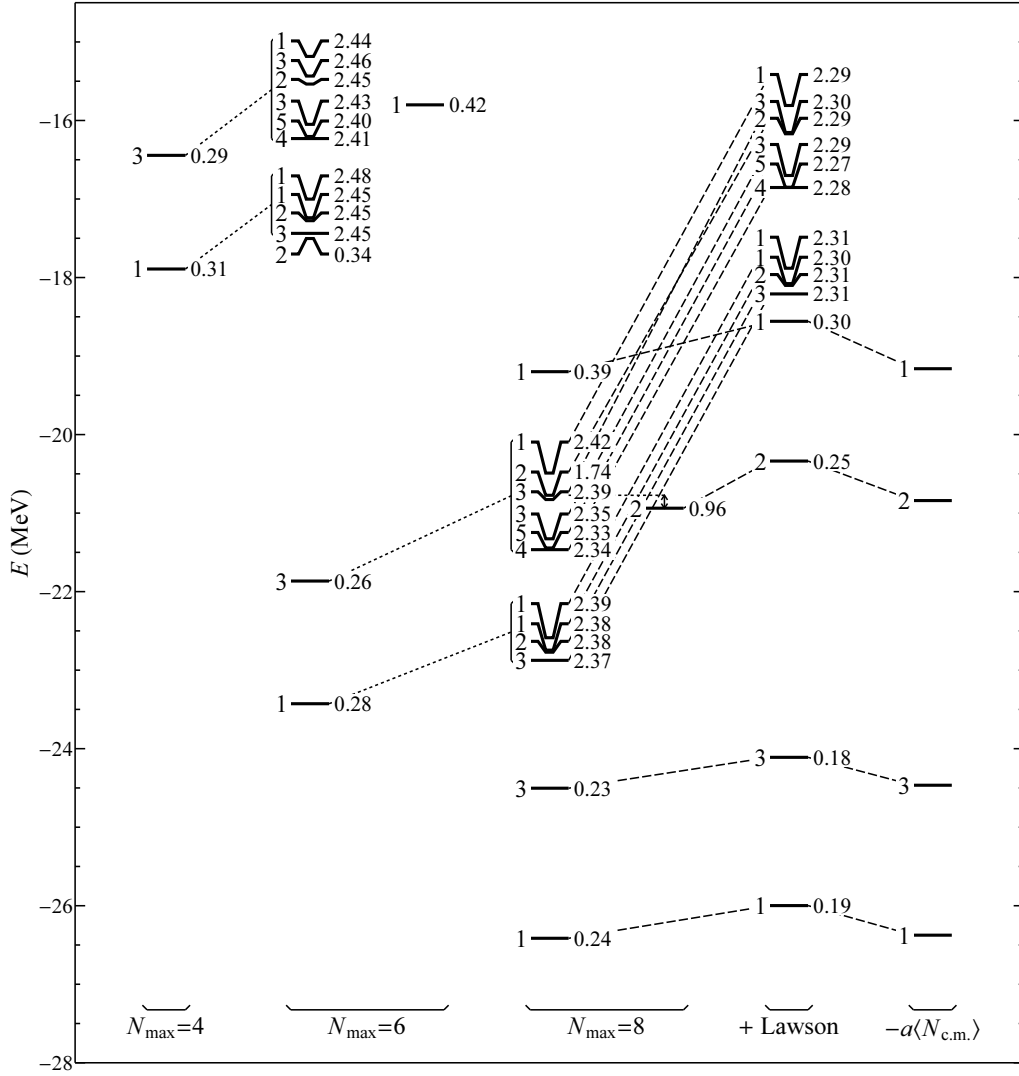


FIG. 9: Level spectrum for ${}^6\text{Li}$, calculated using the Coulomb-Sturmian basis. Calculations (left to right) are for $N_{\text{max}} = 4$, 6, and 8, and then again for $N_{\text{max}} = 8$ with addition of a Lawson term $aN_{\text{c.m.}}^{\Omega_L}$ of strength $a = 2$ MeV. Energies corrected by $-a\langle N_{\text{c.m.}}^{\Omega_L} \rangle$ are shown at far right. For each level, the angular momentum J is indicated at left, and $\langle N_{\text{c.m.}}^{\Omega_L} \rangle$ is indicated at right, as a measure of the number of center-of-mass oscillator quanta. Approximately degenerate multiplets of spurious states are marked by brackets and connected to the state at lower N_{max} to which they are approximately related by coupling to two center-of-mass quanta. The dashed lines trace the change in level energy induced by the Lawson term. For $N_{\text{max}} = 8$, an arrow connects the two $J = 2$ levels which may be described (see text) as admixtures of a nonspurious and spurious level. These calculations are for $\hbar\Omega = 20$ MeV, with $N_{\text{cut}} = 13$. The quantity $\langle N_{\text{c.m.}}^{\Omega_L} \rangle$ is evaluated for $\hbar\tilde{\Omega} = 20$ MeV, and the Lawson term is defined for $\hbar\Omega_L = 20$ MeV as well.

angular momentum $l_{\text{c.m.}}$ and intrinsic angular momentum J_{in} . Recall that the three-dimensional oscillator spectrum contains angular momenta $l = 0$ for $N = 0$, $l = 1$ for $N = 1$, $l = (0, 2)$ for $N = 2$, $l = (1, 3)$ for $N = 3$, $l = (0, 2, 4)$ for $N = 4$, *etc.* Spurious states with $N_{\text{c.m.}} = 1$ lie in the opposite-parity space and therefore do not appear in Fig. 8.¹¹ However, for $N_{\text{c.m.}} = 2$, cou-

pling $l_{\text{c.m.}} = 0$ and 2 to the $J_{\text{in}} = 1$ intrinsic ground state yields a spurious-state multiplet with angular momenta $(3, 2, 1, 1)$, as seen in Fig. 8. Similarly, coupling these values of $l_{\text{c.m.}}$ to the $J_{\text{in}} = 3$ intrinsic excited state yields a spurious-state multiplet with angular momenta $(5, 4, 3, 3, 2, 1)$. The $N_{\text{c.m.}} = 4$ spurious multiplets seen

¹¹ Odd spurious excitations of odd-parity intrinsic states, *e.g.*, in

the $\mathcal{H}_{\text{c.m.}}^1 \otimes \mathcal{H}_{\text{in}}^5$ subspace, do indeed appear in the even-parity spectrum, but in ${}^6\text{Li}$ these are at higher energy.

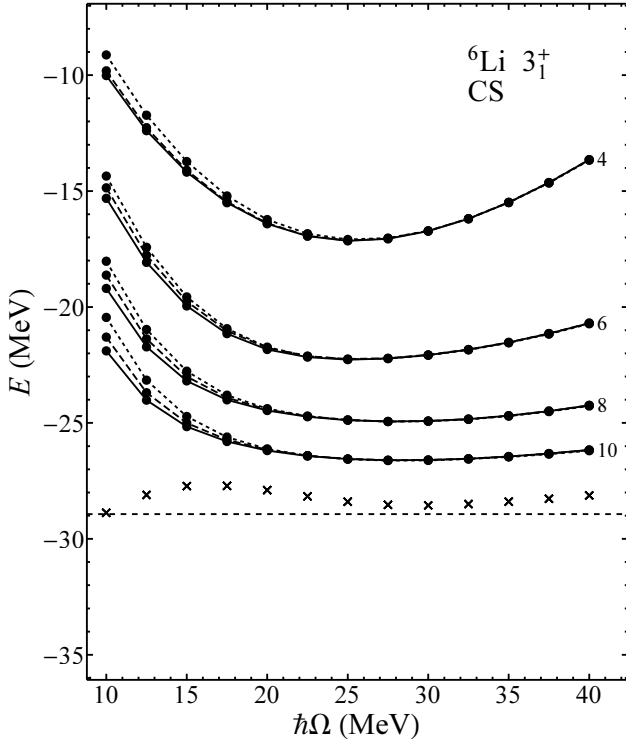


FIG. 10: The ${}^6\text{Li } 3^+$ excited state energy, calculated using the Coulomb-Sturmian basis, as in Fig. 4(d), but now including a Lawson term, with strength $a = 2$ MeV and Lawson term oscillator energy $\hbar\Omega_L$ chosen equal to the basis $\hbar\Omega$. Energies are corrected by subtracting $a\langle N_{\text{c.m.}}^{\Omega_L} \rangle$. See the caption to Fig. 4 for further explanation of curves and symbols.

at $N_{\text{max}} = 8$ in Fig. 8 are obtained similarly by coupling $l_{\text{c.m.}} = 0, 2$, and 4 to the intrinsic state.

It is apparent from Fig. 8 that a high level of contamination of the low-lying spectrum with spurious states will arise with increasing N_{max} , as the difference in energy between intrinsic ground states in successive N_{max} spaces decreases. Already several spurious states arise below the first excited state at $N_{\text{max}} = 8$ in this example. This would become a prohibitive problem for large N_{max} , as suggested in Sec. II C, since the Lanczos diagonalization in the many-body problem must converge the spurious states along with the nonspurious states. However, for the N_{max} -truncated oscillator basis, as noted in Sec. II C, inclusion of the Lawson term in the Hamiltonian pushes the spurious solutions to higher energy, without affecting the nonspurious states, obviating the problem [Fig. 8 (far right)].

With this understanding of the spurious state spectrum for the oscillator basis, we now have a baseline for interpreting the eigenvalue spectrum obtained with a Coulomb-Sturmian basis, shown in Fig. 9 for basis $\hbar\Omega = 20$ MeV. It is seen that the same multiplets of spurious states (marked with brackets in the figure) arise as in the calculation based on the oscillator basis, but now the degeneracies — with the nonspurious state at lower

N_{max} and between the members of the multiplet itself — are only approximate. Since we are using the intrinsic Hamiltonian, these energy differences do not arise from any direct contribution of the center-of-mass dynamics to the energy. Rather, to the extent that factorization occurs, these differences arise from variation in the level of convergence of the intrinsic wavefunction associated with the center-of-mass wavefunction. Alternatively, to the extent that factorization is imperfect, these differences can arise from admixtures of contributions involving different center-of-mass and intrinsic excitations.

Although these states in Fig. 9 are not eigenstates of $N_{\text{c.m.}}^{\Omega}$, we can still calculate an average number of center-of-mass oscillator quanta as $\langle N_{\text{c.m.}}^{\Omega} \rangle$. This expectation is indicated to the right of each level in Fig. 9, where $\hbar\tilde{\Omega}$ has been chosen simply equal to the basis $\hbar\Omega$, *i.e.*, $\hbar\tilde{\Omega} = 20$ MeV. It is seen that the $\langle N_{\text{c.m.}}^{\Omega} \rangle$ values clearly reflect the identification of the states as spurious or non-spurious according to the energy spectrum noted above. The nonspurious states share a similar range of values for $\langle N_{\text{c.m.}}^{\Omega} \rangle$ — at $N_{\text{max}} = 8$, nearly identical for the ground state and first excited state (~ 0.24) and somewhat higher (~ 0.3 – 0.4) for some of the higher states. The states analogous to the $N_{\text{c.m.}} = 2$ spurious states of the oscillator-basis calculation, in contrast, have $\langle N_{\text{c.m.}}^{\Omega} \rangle$ values which cluster closely around 2.4.

Note the two 2^+ states at about -21 MeV in the $N_{\text{max}} = 8$ calculation of Fig. 9. With exact factorization, one of these would be nonspurious and the other spurious. However, the $\langle N_{\text{c.m.}}^{\Omega} \rangle$ values for these two states (~ 0.96 and ~ 1.74) indicate that the spurious and non-spurious states are strongly mixed. This mixing provides an illustration of the challenge associated with contamination of the low-lying spectrum with spurious states. As the density of spurious states increases with N_{max} , the close proximity of spurious and nonspurious states may be expected to lead to extensive mixing and consequently a breakdown of center-of-mass factorization for even the lowest-lying states. Therefore, it is even more important that the spurious states be eliminated from the low-lying spectrum than it is for conventional oscillator basis calculations.

With this in mind, we explore the efficacy of the Lawson term when used with the Coulomb-Sturmian basis. At right in Fig. 9, the effect of introducing a Lawson term $aN_{\text{c.m.}}^{\Omega_L}$ to the Hamiltonian is shown. For simplicity in this illustration, we choose $\hbar\Omega_L = 20$ MeV, corresponding to the basis $\hbar\Omega$ and the $\hbar\tilde{\Omega}$ for the $\langle N_{\text{c.m.}}^{\Omega} \rangle$ values indicated. This choice is arbitrary,¹² and another value,

¹² When used with the oscillator basis, the center-of-mass oscillator energy $\hbar\Omega_L$ in the Lawson operator is generally chosen equal to the basis $\hbar\Omega$, to preserve factorization. However, when used with a general, non-oscillator basis, there is no such requisite pairing, and $\hbar\Omega_L$ may be chosen freely, so as to obtain the most effective removal of spurious dynamics.

such as that at which $\langle N_{\text{c.m.}}^{\Omega_L} \rangle$ is minimized for the ground state, might well be profitably used. A Lawson strength $a = 2$ MeV has been adopted, as sufficiently large to expunge spurious states from the lowest few MeV of the spectrum, but not so large as to place undue weight on coercing the center-of-mass wavefunction into a pure $0s$ oscillator state, at the possible expense of compromising convergence of the intrinsic state. The change of energies with introduction of the Lawson term is traced by dashed lines in Fig. 9. Notice that the mixing of the nonspurious and spurious 2^+ states discussed above (now at energies of about -20 MeV and -16 MeV, respectively) has been eliminated.

The Lawson term is also seen, from the expectation values indicated in Fig. 9, to reduce $\langle N_{\text{c.m.}}^{\Omega_L} \rangle$ for these states. It is not yet clear how much of this change reflects improvement of the center-of-mass factorization and how much simply relects modification of an already-factorized center-of-mass function towards oscillator $0s$ form.

Since even the nonspurious states have nonzero values for $\langle N_{\text{c.m.}}^{\Omega_L} \rangle$, their energies are raised by introduction of the Lawson term, by $\sim a\langle N_{\text{c.m.}}^{\Omega_L} \rangle$. This contribution is *not* expected to vanish in the large N_{max} limit, since $\langle N_{\text{c.m.}}^{\Omega_L} \rangle$ has already been seen not to approach zero. To recover the eigenvalue of the *intrinsic* Hamiltonian on the *intrinsic* wavefunction, to the extent that good factorization is obtained, we must correct the calculated energy for the contribution of the Lawson term acting on the center-of-mass function, by subtracting $a\langle N_{\text{c.m.}}^{\Omega_L} \rangle$ back off. The energies obtained after this correction, for the nonspurious states, are shown at far right in Fig. 9. After correction, the original values for the energies, as obtained before introduction of the Lawson term, are almost (but not quite) recovered. The corrected energies are still marginally higher, likely reflecting the compromise in convergence of the intrinsic state incurred by the Lawson term, and this discrepancy increases with the Lawson strength a used in the calculation.

The Lawson term thus appears to be a credible means of eliminating spurious states from the low-lying spectrum, in calculations with the Coulomb-Sturmian basis. The essential question, if the Lawson term is to be used in practice, is whether or not the Lawson term has any significant adverse impact on convergence properties. Taking the energy of the first excited state as an example, we repeat the calculations of Fig. 4(d), but now including a Lawson term of strength $a = 2$ MeV, resulting in the energies in Fig. 10. The $a\langle N_{\text{c.m.}}^{\Omega_L} \rangle$ correction to the energies, described above, has been included. The results are virtually indistinguishable from those of Fig. 4(d). For comparison with the discussion in Sec. IV B, we note that the convergence rate at the variational minimum ($\hbar\Omega = 30$ MeV) is still $c \approx 0.30$, and the extrapolated energy is still approximately -28.6 MeV.

V. CONCLUSION

Although the conventional oscillator basis has definite advantages for *ab initio* nuclear many-body calculations with the NCCI approach, namely, the potential for exact center-of-mass factorization of eigenstates and the simplicity of the Moshinsky transformation for Hamiltonian matrix elements, it also presents the disadvantage of nonphysical Gaussian asymptotics at large distances, *i.e.*, the oscillator wavefunctions satisfy the wrong boundary conditions at infinity for use with bound states of nuclei. The Coulomb-Sturmian functions retain the advantages of forming a complete, discrete set of square-integrable functions while also exhibiting realistic exponential asymptotics. We have seen that the technical and physical challenges of carrying out NCCI calculations with a Coulomb-Sturmian basis are tractable. To briefly summarize the computational framework, the many-body calculation has the standard structure for an nlj single-particle basis, the interaction matrix elements are transformed from the harmonic-oscillator basis, and relative kinetic energy matrix elements are calculated separately. In the initial exploratory calculations considered here, it is found that the convergence rates for energies are competitive with those obtained with an oscillator basis, the convergence rate for the RMS radius is superior, and spurious center-of-mass excitations can be successfully managed. Many of the considerations addressed in this work could be relevant to NCCI calculations with other possible radial bases as well, *e.g.*, transformed harmonic oscillator bases [40].

The importance of the asymptotic properties of the basis functions may be expected to vary depending upon the physical properties of the nucleus and state under consideration. A basis such as the Coulomb-Sturmian basis might well be particularly appropriate to halo nuclei, where the mismatch with the oscillator functions at large distances is particularly severe. Another case of interest would be states involving clusters with significant spatial separation. The importance of reproducing the large- r properties of the nuclear eigenstates may also be expected to depend upon the observable under consideration, depending upon how heavily large- r contributions are weighted by that observable. Thus, *e.g.*, the difference between Gaussian and exponential asymptotics may be expected to be more important for the RMS radius or $E2$ observables than for $M1$ observables. Asymptotic properties also play a significant role in scattering problems. The extent to which a Coulomb-Sturmian basis may be successfully used in *ab initio* scattering calculations, *e.g.*, through a generalization of the no-core shell model resonating group method (NCSM/RGM) [41], will depend critically upon the details of the center-of-mass factorization properties.

To more fully ascertain the relative advantages or disadvantages of the Coulomb-Sturmian basis for NCCI calculations, extensive and systematic calculations are required, both into the convergence properties of the basis

and the robustness of extrapolations. Most obviously, these need to be carried to high N_{\max} , for a variety of nuclei and interactions. However, there is also considerable room for optimization within the method itself, which must be explored. The prescription for the l -dependence of the length parameter within the single-particle basis (Sec. III B) and the many-body truncation scheme (Sec. IV A), in which the present oscillator-like $N = 2n + l$ “energy” weighting is dictated purely by convenience, are notable areas of possible improvement. Although the two-body JISP16 interaction was used in the illustrative calculations, the transformation procedure (Sec. III C) carries over readily to three-body interactions, so convergence properties with, *e.g.*, chiral effective field theory interactions with similarity renormalization group evolution [42], can be investigated.

Acknowledgments

We thank M. Pervin and W. N. Polyzou for pointing out the relevance of the Coulomb-Sturmian basis. We also thank T. Dytrych for assistance in the validation process, Ch. Constantinou and A. E. McCoy for comments on the manuscript, and T. Papenbrock and S. Quaglioni for valuable discussions. This work was supported by the Research Corporation for Science Advancement through the Cottrell Scholar program, by the US Department of Energy under Grants No. DE-FG02-95ER-40934, DE-FC02-09ER41582 (SciDAC/UNEDF), and DE-FG02-87ER40371, and by the US National Science Foundation under Grant No. 0904782. Computational resources were provided by the National Energy Research Supercomputer Center (NERSC), which is supported by the Office of Science of the U.S. Department of Energy under Contract No. DE-AC02-05CH11231.

Appendix A: Center-of-mass decomposition of r^2 and k^2

The one-body operators $r^2 = \sum_i r_i^2$ and $k^2 = \sum_i k_i^2$, for the A -body system, may be decomposed into separate parts depending only upon the center-of-mass coordinate (or momentum) and on the relative coordinates (or momenta), respectively. The decompositions of the kinetic energy operator T and noninteracting harmonic oscillator potential U into center-of-mass and relative parts follow immediately. In this appendix, we summarize the relations among relative and center-of-mass operators, both for reference in the present discussion and to establish a uniform notation for the description of coordinate-space and momentum-space matrix elements in Sec. III D.

Recall that the center-of-mass coordinate and momentum vectors are

$$\mathbf{R} = \frac{1}{A} \sum_i \mathbf{r}_i \quad \mathbf{P} = \sum_i \mathbf{p}_i. \quad (\text{A1})$$

In the following, we let $\mathbf{p}_i = \hbar \mathbf{k}_i$, $\mathbf{P} = \hbar \mathbf{K}$, *etc.*

First, consider the one-body r^2 operator, defined by

$$r^2 = \sum_i r_i^2. \quad (\text{A2})$$

Comparing the sum on the right hand side of (A2) with those in the operators¹³

$$\begin{aligned} A^2 R^2 &= \left(\sum_i \mathbf{r}_i \right)^2 = \sum_i r_i^2 + \sum_{ij}' \mathbf{r}_i \cdot \mathbf{r}_j, \\ A^2 r_{\text{rel}}^2 &= \frac{1}{2} \sum_{ij}' (\mathbf{r}_i - \mathbf{r}_j)^2 = (A-1) \sum_i r_i^2 - \sum_{ij}' \mathbf{r}_i \cdot \mathbf{r}_j. \end{aligned} \quad (\text{A3})$$

demonstrates that

$$A r^2 = A^2 R^2 + A^2 r_{\text{rel}}^2. \quad (\text{A4})$$

Multiplying by $(m\Omega^2)/(2A)$ gives the decomposition of the harmonic oscillator potential energy operator U^Ω into center-of-mass and relative contributions, $U^\Omega = U_{\text{c.m.}}^\Omega + U_{\text{rel}}^\Omega$, where

$$\begin{aligned} U_{\text{c.m.}}^\Omega &= \frac{m\Omega^2}{2A} (A^2 R^2), \quad U_{\text{rel}}^\Omega = \frac{m\Omega^2}{2A} (A^2 r_{\text{rel}}^2), \\ U^\Omega &= \frac{m\Omega^2}{2A} (A r^2). \end{aligned} \quad (\text{A5})$$

The quantity r_{rel}^2 has the geometric significance that it is the mean square radius relative to the center of mass, *i.e.*,

$$r_{\text{rel}}^2 = \frac{1}{A} \sum_i (\mathbf{r}_i - \mathbf{R})^2. \quad (\text{A6})$$

The square root of the expectation value of this operator, $\langle r_{\text{rel}}^2 \rangle^{1/2}$, is the point-nucleon RMS radius.

Similarly, consider the one-body k^2 operator, defined by

$$k^2 = \sum_i k_i^2. \quad (\text{A7})$$

Comparison with the sums in

$$\begin{aligned} K^2 &= \left(\sum_i \mathbf{k}_i \right)^2 = \sum_i k_i^2 + \sum_{ij}' \mathbf{k}_i \cdot \mathbf{k}_j, \\ k_{\text{rel}}^2 &= \frac{1}{2} \sum_{ij}' (\mathbf{k}_i - \mathbf{k}_j)^2 = (A-1) \sum_i k_i^2 - \sum_{ij}' \mathbf{k}_i \cdot \mathbf{k}_j, \end{aligned} \quad (\text{A8})$$

¹³ We include the factors of A^2 on the left hand side of (A3) as compensation for the factor of $1/A$ appearing in the definition (A1) of \mathbf{R} , so as to simplify the right hand side. In particular, this maintains the parallel with the decomposition of momentum space operators in (A8)

demonstrates that

$$Ak^2 = K^2 + k_{\text{rel}}^2. \quad (\text{A9})$$

Multiplying by $\hbar^2/(2Am_N)$ gives us the decomposition of the kinetic energy operator T into center-of-mass and relative contributions, $T = T_{\text{c.m.}} + T_{\text{rel}}$, where

$$\begin{aligned} T_{\text{c.m.}} &= \frac{(\hbar^2 K^2)}{2Am_N}, \quad T_{\text{rel}} = \frac{(\hbar^2 k_{\text{rel}}^2)}{2Am_N}, \\ T &= \frac{(A\hbar^2 k^2)}{2Am_N}. \end{aligned} \quad (\text{A10})$$

Appendix B: Zeros of generalized Laguerre and Jacobi polynomials

Numerically robust evaluation of the radial integrals which arise in evaluation of the overlaps between harmonic oscillator and Coulomb-Sturmian bases (Sec. III C) and the radial matrix elements for the Coulomb-Sturmian basis (Sec. III D) requires accurate knowledge of the zeros of the integrands in (40)–(41), (49)–(50), and (58)–(59), thus of generalized Laguerre polynomials $L_n^\alpha(x)$ and Jacobi polynomials $J_n^{(\alpha,\beta)}(x)$. Although, in principle, generic numerical rootfinding algorithms may be used, it is preferable to determine the zeros according to a more reliable and efficient approach specific to orthogonal polynomials, such as the Golub-Welch algorithm [43]. This method requires recurrence coefficients for the relevant *monic* polynomials, *i.e.*, such that the highest-order coefficient is unity, as summarized in this appendix.

The Golub-Welch algorithm is specifically formulated for monic polynomials. Consider a family of polynomials $p_n(x) = \sum_{m=0}^n c_m x^m$ ($n = 0, 1, \dots$), orthogonal under weight function $w(x)$ on the interval $[a, b]$, and with $c_n = 1$. Suppose these polynomials satisfy the recurrence relation

$$p_{n+1}(x) + (B_n - x)p_n(x) + A_n p_{n-1}(x) = 0, \quad (\text{B1})$$

characterized by recurrence coefficients A_n and B_n . Then, to find the zeros p_n via the Golub-Welch algorithm [43], one must construct the corresponding Jacobi matrix J . This is the $n \times n$ tridiagonal matrix consisting of entries $J_{i,i} = B_{i-1}$ on the main diagonal and $J_{i-1,i} = J_{i,i-1} = (A_{i-1})^{1/2}$ on the adjacent diagonals. As a tridiagonal matrix, J is easily diagonalized. The eigenvalues x_i , for $i = 1, 2, \dots, n$, are then the zeros of p_n .

The generalized Laguerre polynomials L_n^α are not monic, having $c_n = (-)^n n!$ [28]. We must therefore instead consider the *monic* generalized Laguerre polynomials \hat{L}_n^α , defined by $\hat{L}_n^\alpha(x) = (-)^n n! L_n^\alpha(x)$ [44]. These satisfy a recurrence relation of the form (B1), with recurrence coefficients

$$\begin{aligned} A_n &= n(n + \alpha) \\ B_n &= 2n + \alpha + 1. \end{aligned} \quad (\text{B2})$$

The Jacobi polynomials $P_n^{(\alpha,\beta)}$ are likewise not monic, having $c_n = 2^{-n} \binom{2n+\alpha+\beta}{n}$ [28]. We must therefore instead consider the *monic* Jacobi polynomials $\hat{P}_n^{(\alpha,\beta)}$, defined by $\hat{P}_n^{(\alpha,\beta)}(x) = 2^n \binom{2n+\alpha+\beta}{n}^{-1} P_n^{(\alpha,\beta)}(x)$ [44]. These satisfy a recurrence relation of the form (B1), now with

$$\begin{aligned} A_n &= \frac{4n(n + \alpha)(n + \beta)(n + \alpha + \beta)}{(2n + \alpha + \beta)^2(2n + \alpha + \beta + 1)(2n + \alpha + \beta - 1)} \\ B_n &= \frac{\beta^2 - \alpha^2}{(2n + \alpha + \beta)(2n + \alpha + \beta + 2)}. \end{aligned} \quad (\text{B3})$$

The Golub-Welch algorithm also yields the weights w_i appearing in the n -point Gaussian integration formula associated with this family of polynomials, $\int_a^b f(x)w(x)dx \approx \sum_{i=1}^n f(x_i)w_i$, which are obtained from the eigenvectors of J , as detailed in Ref. [43]. The zeros and weights appearing in n -point Gauss-Legendre quadrature formulas used in evaluating the radial integrals of Sec. III are widely tabulated [28]. However, it is convenient to note that the Jacobi matrix required in obtaining these may also be obtained using the recurrence coefficients of (B3). It is necessary to consider the monic Legendre polynomials $\hat{P}_n(x) = [2^n(n!)/(2n)!]P_n(x)$ [44], which constitute a special case of the monic Jacobi polynomials, $\hat{P}_n(x) = \hat{P}_n^{(0,0)}(x)$, described by (B3) with $\alpha = \beta = 0$.

Appendix C: Two-body states

In this appendix, the notation is established for the *antisymmetrized* (AS) and *normalized antisymmetrized* (NAS) two-particle states, with angular momentum coupling. These definitions are required for discussion of like-particle two-body matrix elements in Sec. III.

We first define angular momentum coupled states

$$|ab; J\rangle = \sum_{m_a m_b} (j_a m_a j_b m_b | JM) |a m_a\rangle |b m_b\rangle. \quad (\text{C1})$$

for two *distinguishable* particles, that is, particle 1 is in orbital a , and particle 2 is in orbital b . We denote such distinguishable-particle states by using parentheses rather than angle brackets, following the conventions of Ref. [29]. Such states may be used directly for the case of one proton and one neutron, *i.e.*,

$$|ab; J\rangle_{pn} = \sum_{m_a m_b} (j_a m_a j_b m_b | JM) |a m_a\rangle_p |b m_b\rangle_n. \quad (\text{C2})$$

However, for two *like* fermions, *antisymmetrized* states are then obtained as

$$\begin{aligned} |ab; JM\rangle_{\text{AS}} &\equiv (c_a^\dagger \times c_b^\dagger)_M^J | \rangle \\ &= \frac{1}{\sqrt{2}} [|ab; JM\rangle - (-)^{J-j_a-j_b} |ba; JM\rangle]. \end{aligned} \quad (\text{C3})$$

These states have the basic symmetry property

$$|ab; JM\rangle_{\text{AS}} = -(-)^{J-j_a-j_b}|ba; JM\rangle_{\text{AS}}. \quad (\text{C4})$$

Therefore, if the orbitals a and b are identical, only states with J even may be obtained. The states defined in (C3) are antisymmetrized but not strictly normalized, in that a further factor of $1/\sqrt{2}$ is required for normalization in the special case in which both particles occupy the same orbital. Strict normalization, even in this special case, is obtained by taking *normalized antisymmetrized* (NAS) states

$$|ab; JM\rangle_{\text{NAS}} = (1 + \delta_{ab})^{-1/2}|ab; JM\rangle_{\text{AS}}. \quad (\text{C5})$$

Two-body matrix elements may be represented in either the AS scheme or NAS scheme, with the relation

$$\begin{aligned} \langle cd; J|V|ab; J\rangle_{\text{NAS}} \\ = (1 + \delta_{cd})^{-1/2}(1 + \delta_{ab})^{-1/2}\langle cd; J|V|ab; J\rangle_{\text{AS}}, \end{aligned} \quad (\text{C6})$$

shown here for matrix elements of a scalar operator V within a single J -space. Both schemes are in common use for representing interaction matrix elements. The AS scheme may yield simpler expressions than the NAS scheme, *e.g.*, as seen comparing the change of basis relation (45) with (46).

Appendix D: Rescaling of separable matrix elements

For the separable calculation of matrix elements described in Sec. IIID, the relations (61) provide A -dependent expressions for the two-body matrix elements of R^2 , r_{rel}^2 , K^2 , and k_{rel}^2 in terms of the A -independent two-body matrix elements $\langle cd; J|V_{r^2}|ab; J\rangle$, $\langle cd; J|V_{\mathbf{r}_1 \cdot \mathbf{r}_2}|ab; J\rangle$, $\langle cd; J|V_{k^2}|ab; J\rangle$, and $\langle cd; J|V_{\mathbf{k}_1 \cdot \mathbf{k}_2}|ab; J\rangle$. These matrix elements still depend on the length parameter chosen for the basis. However, the operators V_{r^2} and $V_{\mathbf{r}_1 \cdot \mathbf{r}_2}$ are homogeneous of order 2 in the coordinates, *i.e.*, their matrix elements scale with the length parameter as b^2 , and the operators V_{k^2} and $V_{\mathbf{k}_1 \cdot \mathbf{k}_2}$ are homogeneous of order -2 , *i.e.*, their matrix elements scale as b^{-2} . Recall that, under the prescription of Sec. IIIB, the length parameters b_l appearing in all Coulomb-Sturmian functions are proportional to a common length parameter b_{HO} (this common proportionality is a general property to be expected of any prescription for the b_l). Therefore, these matrix elements of V_{r^2} , $V_{\mathbf{r}_1 \cdot \mathbf{r}_2}$, V_{k^2} , and $V_{\mathbf{k}_1 \cdot \mathbf{k}_2}$ need only be calculated once, at some particular reference value for the length scale, and then may be transformed to the actual length scale, or $\hbar\Omega$ value, of the many-body calculation by simple multiplication. For evaluation of the radial integrals appearing in (49), (50), (58), and (59), it is natural to adopt a dimensionless reference scale $b_{\text{HO}} = 1$. Thus it is only necessary to evaluate matrix elements $\langle cd; J|V_{r^2}|ab; J\rangle_0$, $\langle cd; J|V_{\mathbf{r}_1 \cdot \mathbf{r}_2}|ab; J\rangle_0$, $\langle cd; J|V_{k^2}|ab; J\rangle_0$,

and $\langle cd; J|V_{\mathbf{k}_1 \cdot \mathbf{k}_2}|ab; J\rangle_0$, by which we denote matrix elements evaluated at $b_{\text{HO}} = 1$. In this appendix, we give explicit expressions for matrix elements of physically relevant operators, for a given basis $\hbar\Omega$, in terms of these reference matrix elements and dimensional scale factors.

Two-body matrix elements of the relative kinetic energy are given by

$$\begin{aligned} \langle cd; J|T_{\text{rel}}|ab; J\rangle &= \left(\frac{\hbar\Omega}{2A}\right)\langle cd; J|V_{k^2}|ab; J\rangle_0 \\ &\quad - 2\left(\frac{\hbar\Omega}{2A}\right)\langle cd; J|V_{\mathbf{k}_1 \cdot \mathbf{k}_2}|ab; J\rangle_0 \end{aligned} \quad (\text{D1})$$

and those of the r_{rel}^2 observable by

$$\begin{aligned} \langle cd; J|r_{\text{rel}}^2|ab; J\rangle &= \left(\frac{b_{\text{HO}}^2}{A^2}\right)\langle cd; J|V_{r^2}|ab; J\rangle_0 \\ &\quad - 2\left(\frac{b_{\text{HO}}^2}{A^2}\right)\langle cd; J|V_{\mathbf{r}_1 \cdot \mathbf{r}_2}|ab; J\rangle_0. \end{aligned} \quad (\text{D2})$$

For present purposes, it is most convenient to reexpress b_{HO} in terms of $\hbar\Omega$ using combinations of physical constants chosen so as to only involve energy and length units, as

$$b_{\text{HO}} = \frac{(\hbar c)}{[(m_N c^2)(\hbar\Omega)]^{1/2}}, \quad (\text{D3})$$

where $m_N c^2 \approx 938.92$ MeV and $\hbar c \approx 197.327$ MeV fm.

In the investigation of center-of-mass separation and in the Lawson term as applied to NCCI calculations with the Coulomb-Sturmian basis (Sec. IV D), we consider the center-of-mass oscillator number operator $N_{\text{c.m.}}^{\tilde{\Omega}}$ of (63), involving an arbitrary oscillator energy $\hbar\tilde{\Omega}$, in general different from the basis $\hbar\Omega$. This operator has two-body matrix elements

$$\begin{aligned} \langle cd; J|N_{\text{c.m.}}^{\tilde{\Omega}}|ab; J\rangle &= \\ \frac{1}{2A} \frac{(\hbar\Omega)}{(\hbar\tilde{\Omega})} &\left[\frac{1}{A-1} \langle cd; J|V_{k^2}|ab; J\rangle_0 + 2 \langle cd; J|V_{\mathbf{k}_1 \cdot \mathbf{k}_2}|ab; J\rangle_0 \right] \\ + \frac{1}{2A} \frac{(\hbar\tilde{\Omega})}{(\hbar\Omega)} &\left[\frac{1}{A-1} \langle cd; J|V_{r^2}|ab; J\rangle_0 + 2 \langle cd; J|V_{\mathbf{r}_1 \cdot \mathbf{r}_2}|ab; J\rangle_0 \right] \\ &\quad - \frac{3}{A(A-1)} \langle cd; J|\mathbb{1}_{2b}|ab; J\rangle, \end{aligned} \quad (\text{D4})$$

where $\mathbb{1}_{2b}$ is the identity operator on the two-body space. If one is evaluating $\langle N_{\text{c.m.}}^{\tilde{\Omega}} \rangle$ for several values of $\hbar\tilde{\Omega}$, as in Fig. 7, it suffices to calculate the expectation values of just the two operators P^2 and R^2 for the many-body state, since these two numerical values may then be combined arithmetically by (63) to deduce $\langle N_{\text{c.m.}}^{\tilde{\Omega}} \rangle$ for any value of $\hbar\tilde{\Omega}$. More simply, in terms of the expectation values of the dimensionless operators $K_0^2 = P^2/(m_N \hbar\Omega)$ and $A^2 R_0^2 = (m_N \Omega A^2/\hbar) R^2$, corresponding to the two-body matrix elements appearing in brackets, respectively,

in (D4), we have

$$\langle N_{\text{c.m.}}^{\tilde{\Omega}} \rangle = \frac{1}{2A} \frac{(\hbar\tilde{\Omega})}{(\hbar\Omega)} \langle K_0^2 \rangle + \frac{1}{2A} \frac{(\hbar\tilde{\Omega})}{(\hbar\Omega)} \langle A^2 R_0^2 \rangle - \frac{3}{2}. \quad (\text{D5})$$

The number operator $N^{\tilde{\Omega}}$ for the one-body harmonic oscillator Hamiltonian $H^{\tilde{\Omega}}$, though not used in the present work, can also be of interest. For instance, if a many-body state has been obtained from an NCCI calculation using the Coulomb-Sturmian basis, $\langle N^{\Omega} \rangle$ provides an estimate of the number of quanta which would be required to represent this same state in a space spanned by a conventional harmonic-oscillator basis of oscillator en-

ergy $\hbar\Omega$, or a Hamiltonian term proportional to N^{Ω} may be used for calculations involving an external harmonic oscillator trapping field. The two-body matrix elements are given by

$$\begin{aligned} \langle cd; J | N^{\tilde{\Omega}} | ab; J \rangle &= \frac{1}{2(A-1)} \frac{(\hbar\tilde{\Omega})}{(\hbar\Omega)} \langle cd; J | V_{k^2} | ab; J \rangle_0 \\ &+ \frac{1}{2(A-1)} \frac{(\hbar\tilde{\Omega})}{(\hbar\Omega)} \langle cd; J | V_{r^2} | ab; J \rangle_0 \\ &- \frac{3}{A-1} \langle cd; J | \mathbb{1}_{2b} | ab; J \rangle. \quad (\text{D6}) \end{aligned}$$

-
- [1] D. R. Entem and R. Machleidt, Phys. Rev. C **68**, 041001 (2003).
 - [2] E. Epelbaum, H.-W. Hammer, and U.-G. Meißner, Rev. Mod. Phys. **81**, 1773 (2009).
 - [3] P. Navrátil, J. P. Vary, and B. R. Barrett, Phys. Rev. Lett. **84**, 5728 (2000); Phys. Rev. C **62**, 054311 (2000).
 - [4] M. Rotenberg, Ann. Phys. (N.Y.) **19**, 262 (1962).
 - [5] E. J. Weniger, J. Math. Phys. **26**, 276 (1985).
 - [6] E. A. Hylleraas, Z. Phys. **48**, 469 (1928).
 - [7] P.-O. Löwdin and H. Shull, Phys. Rev. **101**, 1730 (1956).
 - [8] M. Rotenberg, Adv. At. Mol. Phys. **6**, 233 (1970).
 - [9] S. Jacobs, M. G. Olsson, and C. Suchyta, III, Phys. Rev. D **33**, 3338 (1986).
 - [10] L. P. Fulcher, Z. Chen, and K. C. Yeong, Phys. Rev. D **47**, 4122 (1993).
 - [11] B. D. Keister and W. N. Polyzou, J. Comput. Phys. **134**, 231 (1997).
 - [12] M. Pervin, Ph.D. thesis, Florida State University (2005).
 - [13] C. Forssen, J. P. Vary, E. Caurier, and P. Navratil, Phys. Rev. C **77**, 024301 (2008).
 - [14] P. Maris, J. P. Vary, and A. M. Shirokov, Phys. Rev. C **79**, 014308 (2009).
 - [15] S. A. Coon, M. I. Avetian, M. K. G. Kruse, U. van Kolck, P. Maris, and J. P. Vary, arXiv:1205.3230v1.
 - [16] M. Moshinsky and Y. F. Smirnov, *The Harmonic Oscillator in Modern Physics* (Harwood Academic Publishers, Amsterdam, 1996).
 - [17] K. T. R. Davies, S. J. Krieger, and M. Baranger, Nucl. Phys. **84**, 545 (1966).
 - [18] M. A. Caprio, P. Maris, and J. P. Vary, J. Phys. Conf. Ser. (submitted).
 - [19] S. Flügge, *Practical Quantum Mechanics I, Grundlehren der mathematischen Wissenschaften* Vol. 177 (Springer-Verlag, Berlin, 1971).
 - [20] D. H. Gloeckner and R. D. Lawson, Phys. Lett. B **53**, 313 (1974).
 - [21] J. P. Elliott and T. H. R. Skyrme, Proc. R. Soc. London A **232**, 561 (1955).
 - [22] C. Lanczos, J. Res. Natl. Bur. Stand. **45**, 255 (1950).
 - [23] A. Messiah, *Quantum Mechanics* (Dover, Mineola, New York, 1999).
 - [24] J. Suhonen, *From Nucleons to Nucleus* (Springer-Verlag, Berlin, 2007).
 - [25] G. B. Arfken and H. J. Weber, *Mathematical Methods for Physicists*, 4th ed. (Academic Press, San Diego, 1995).
 - [26] E. Filter and E. O. Steinborn, J. Math. Phys. **21**, 2725 (1980).
 - [27] B. Klahn and W. A. Bingel, Theoret. Chim. Acta **44**, 27 (1977).
 - [28] F. W. J. Olver, D. W. Lozier, R. F. Boisvert, and C. W. Clark, eds., *NIST Handbook of Mathematical Functions* (Cambridge University Press, Cambridge, 2010).
 - [29] J. W. Negele and H. Orland, *Quantum Many-Particle Systems* (Addison-Wesley, Redwood City, CA, 1988).
 - [30] A. R. Edmonds, *Angular Momentum in Quantum Mechanics*, 2nd ed., Investigations in Physics No. 4 (Princeton University Press, Princeton, New Jersey, 1960).
 - [31] P. Sternberg, E. G. Ng, C. Yang, P. Maris, J. P. Vary, M. Sosonkina, and H. V. Le, in *SC '08: Proceedings of the 2008 ACM/IEEE Conference on Supercomputing* (IEEE Press, Piscataway, NJ, 2008), Article No. 15.
 - [32] J. P. Vary, P. Maris, E. Ng, C. Yang, and M. Sosonkina, J. Phys. Conf. Ser. **180**, 012083 (2009).
 - [33] P. Maris, M. Sosonkina, J. P. Vary, E. Ng, and C. Yang, Procedia Comput. Sci. **1**, 97 (2010).
 - [34] A. M. Shirokov, J. P. Vary, A. I. Mazur, and T. A. Weber, Phys. Lett. B **644**, 33 (2007).
 - [35] C. Cockrell, J. P. Vary, and P. Maris, Phys. Rev. C (submitted), arXiv:1201.0724v1.
 - [36] S. K. Bogner, R. J. Furnstahl, P. Maris, R. J. Perry, A. Schwenk, and J. Vary, Nucl. Phys. A **801**, 21 (2008).
 - [37] H. J. Lipkin, Phys. Rev. **110**, 1395 (1958).
 - [38] G. Hagen, T. Papenbrock, and D. J. Dean, Phys. Rev. Lett. **103**, 062503 (2009); G. Hagen, T. Papenbrock, D. J. Dean, and M. Hjorth-Jensen, Phys. Rev. C **82**, 034330 (2010).
 - [39] J. B. McGrory and B. H. Wildenthal, Phys. Lett. B **60**, 5 (1975).
 - [40] M. V. Stoitsov, W. Nazarewicz, and S. Pittel, Phys. Rev. C **58**, 2092 (1998).
 - [41] S. Quaglioni and P. Navrátil, Phys. Rev. C **79**, 044606 (2009).
 - [42] S. K. Bogner, R. J. Furnstahl, and R. J. Perry, Phys. Rev. C **75**, 061001 (2007).
 - [43] G. H. Golub and J. H. Welsch, Math. Comput. **23**, 221 (1969).
 - [44] A. Cuyt, V. B. Petersen, B. Verdonk, H. Waadeland, and W. B. Jones, *Handbook of Continued Fractions for Special Functions* (Springer-Verlag, Berlin, 2008).